Environmental Surfaces and Interfaces 4 (2026) 98–112

Contents lists available at ScienceDirect

Environmental Surfaces and Interfaces

journal homepage: www.keaipublishing.com/ESI

Waste-derived carbon materials for high-efficiency lithium-ion batteries: A review

Abdulafeez O. Orilonise[a], Kingsley O. Iwuozor[b], Ebuka Chizitere Emenike[b], Joshua Emeghai[c,d], Adewale George Adeniyi[e,*]

[a] Department of Mechanical Engineering, Faculty of Engineering and Technology, University of Ilorin, Ilorin P. M. B. 1515, Nigeria
[b] Department of Pure and Industrial Chemistry, Nnamdi Azikiwe University, Awka P. M. B. 5025, Nigeria
[c] Department of Structural Engineering, University of Benin, Benin-City, Nigeria
[d] Department of Construction Management, Louisiana State University, Baton Rouge, United States
[e] Department of Chemical Engineering, Faculty of Engineering and Technology, University of Ilorin, Ilorin P. M. B. 1515, Nigeria

ARTICLE INFO

Keywords:
Activated carbon
Biochar
Energy storage and conversion
Plastic recycling
Sustainable electrodes

ABSTRACT

Waste derived carbon materials have advanced as sustainable alternatives to graphite for lithium ion battery anodes, yet existing studies remain fragmented because biomass and plastic wastes are often examined separately. This review integrates these research streams and establishes a unified framework linking feedstock composition, co-carbonization behaviour, activation pathways, heteroatom doping, and microstructural evolution to electrochemical performance. The analysis demonstrates that blended biomass-plastic feedstocks generate synergistic effects that shape yield, porosity, interlayer spacing, defect density, and surface chemistry. These structural features govern dual lithium storage mechanisms involving pseudocapacitive adsorption at defect sites and intercalation within turbostratic microdomains. Reported capacities frequently exceed 500 mAh g^{-1} with superior rate performance compared to graphite. The review shows that excessive surface area and uncontrolled activation reduce initial coulombic efficiency through extensive solid electrolyte interphase formation, whereas moderated activation and controlled defect engineering improve cyclability. The study also shows the performance gains achieved by forming hybrids with metal oxides, silicon, and MXenes, which enhance conductivity, buffer volume change, and accelerate ion transport, delivering capacities between 700 and 1200 mAh g^{-1}. Key barriers include low initial coulombic efficiency, variable feedstock quality, and the limited scalability of chemical activation. The review identifies targeted pre-lithiation, multi heteroatom co doping, and data driven synthesis optimisation as essential strategies for advancing waste derived carbons toward commercial anode applications.

1. Introduction

Lithium-ion batteries (LIBs) are the backbone of modern energy storage; they power electric vehicles, portable electronics, and renewable energy systems [1]. Carbon is the most widely used anode material because it offers electrical conductivity, stability, and structural integrity [2]. Graphite dominates commercial use, but its theoretical capacity of 372 mAh/g limits energy density [3]. Furthermore, the production of battery grade graphite is energy-intensive, and its supply chain is geographically concentrated, raising significant environmental and strategic concerns. It also faces safety issues at high charge rates due to lithium plating [4]. Its rigid structure restricts ion transport and limits fast-charging performance [5]. Synthetic carbon materials, while common, involve expensive precursors and energy-intensive processes. Their production adds to the carbon footprint of the battery industry [6]. The search for sustainable, high-capacity alternatives is therefore not merely an academic pursuit but a commercial and environmental imperative. This has driven research toward alternative carbon forms with higher storage capacity and better cycling stability. Waste derived carbon, with its porous structure and tunable surface chemistry, offers a promising route [7–9]. When derived from sustainable feedstocks, it reduces reliance on fossil-based resources and helps manage waste streams [10–12]. Both biomass and plastic wastes are abundant, globally distributed [13,14], and represent a negative-cost feedstock, fundamentally altering the economic and environmental calculus of anode production. More importantly, these precursors produce hard carbons,

* Corresponding author.
E-mail address: adeniyi.ag@unilorin.edu.ng (A.G. Adeniyi).

https://doi.org/10.1016/j.esi.2026.01.001
Received 30 October 2025; Received in revised form 30 November 2025; Accepted 1 January 2026
Available online 2 January 2026
2949-8643/© 2026 The Authors. Publishing services by Elsevier B.V. on behalf of KeAi Communications Co. Ltd. This is an open access article under the CC BY-NC-ND license (http://creativecommons.org/licenses/by-nc-nd/4.0/).

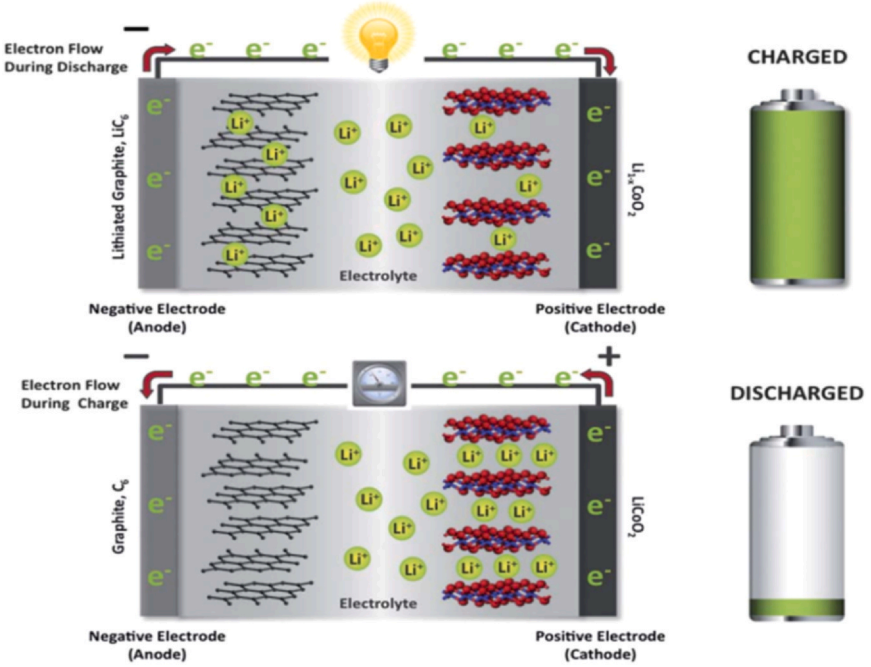


Fig. 1. Schematic illustration of the operation mechanism of lithium-ion batteries [20].

which are structurally distinct from graphite. Unlike graphite's highly ordered crystalline lattice, hard carbons possess a disordered, turbostratic structure characterized by a mix of graphitic microdomains, expanded interlayer spacing ($d_{002} > 0.34$ nm), and abundant micropores [5]. This disordered architecture is a critical feature, not a flaw. It facilitates novel Li-ion storage mechanisms beyond simple intercalation. The characteristic sloping voltage profile of hard carbons (approx. 1.2–0.1 V vs Li/Li^+) corresponds to Li-ion storage at defect sites, heteroatom-doped edges, and via adsorption in nanopores. This is complemented by a low-voltage plateau region (at < 0.1 V) associated with intercalation and pore-filling, which collectively enables reversible capacities far exceeding the graphitic limit, with values reported well over 500 mAh/g [15]. Fig. 1 shows the operation of the lithium-ion mechanism during charge and discharge.

Several review papers have examined waste-derived carbons in energy storage, but each with a narrow scope. Molaiyan et al. [16] studied biomass-derived carbons for lithium-ion and sodium-ion batteries, linking biomass residues, carbon structures, and electrochemical behaviour, but ignored plastics and blended feedstocks. Jin et al. [17] reviewed biomass-based materials for lithium secondary batteries, covering anodes, cathodes, separators, and binders, but stayed focused on biomass alone without considering co-processing with plastics. Ma et al. [18] reviewed plastic waste-derived carbons, showing their use in energy storage, remediation, and synthesis, but did not address integration with biomass or specific use in lithium-ion anodes. Yaqoob et al. [19] analyzed plastic waste conversion to carbon nanomaterials for supercapacitors, discussing processing routes and environmental drivers, but gave little attention to lithium-ion systems or blending with biomass. Together these works show progress on biomass carbons and plastic carbons separately but remain fragmented. They do not explain how blending ratios affect structure, porosity, conductivity, or electrochemical performance. They do not connect feedstock diversity and synthesis methods to cycle stability, rate behaviour, or scalability. This gap leaves limited guidance on moving from isolated studies to integrated strategies. This review addresses this gap by examining synergies, and linking feedstock choice to electrochemical outcomes in lithium-ion batteries.

This review, therefore, moves beyond a simple compilation. Its primary objective is to critically analyze and synthesize the current understanding of waste-derived carbon materials, with a special focus on blended biomass-plastic systems, for LIB anodes. This study first dissects the roles of feedstock selection and synthesis methodologies in tailoring the physicochemical properties of the carbons. Subsequently, it critically correlates these properties (surface area, defect density, heteroatom content) with electrochemical outcomes (capacity, Initial Coulombic Efficiency (ICE), rate capability). Also, the study provides a detailed mechanistic analysis of the unique Li-ion storage pathways in these disordered materials. The novelty is in linking waste management with electrochemical function in one framework and in emphasizing blended systems that past studies treated separately.

Finally, the study identifies the most significant challenges hindering practical application, chiefly low ICE and scalability, and map out future research directions, including the development of advanced hybrid composites and the integration of AI-guided materials design. This review provides both researchers and industry with a practical reference on sustainable carbons for lithium-ion batteries.

2. Feedstock selection and pre-treatment

The electrochemical performance of a waste-derived carbon anode is not a product of chance; it is a direct and traceable consequence of the atomic-level composition of its precursor. The selection of a feedstock, or a blend of feedstocks, is the single most important decision in the synthesis process, as it defines the initial elemental ratios (Carbon (C), Hydrogen (H), Oxygen (O), Nitrogen (N)), the inherent structural propensities (aromatic vs. aliphatic), and the presence of inorganic catalysts (ash) that will govern the material's transformation under thermal treatment.

2.1. Biomass feedstocks

Lignocellulosic biomass, the most abundant and sustainable carbon precursor on Earth, is a composite of three primary polymers: lignin, cellulose, and hemicellulose. The ratio of these components, dictated by

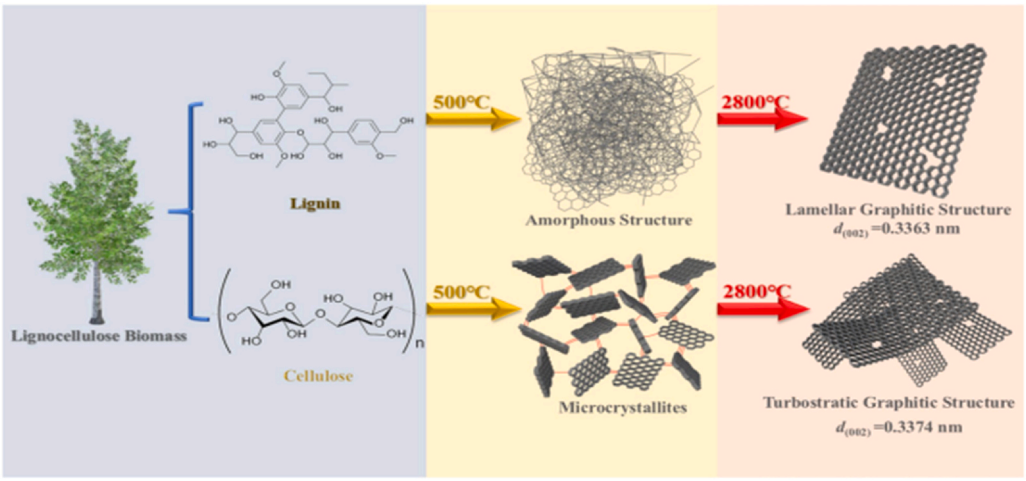


Fig. 2. Structure of biochar derived from lignin and cellulose during graphitization under high temperature. [23].

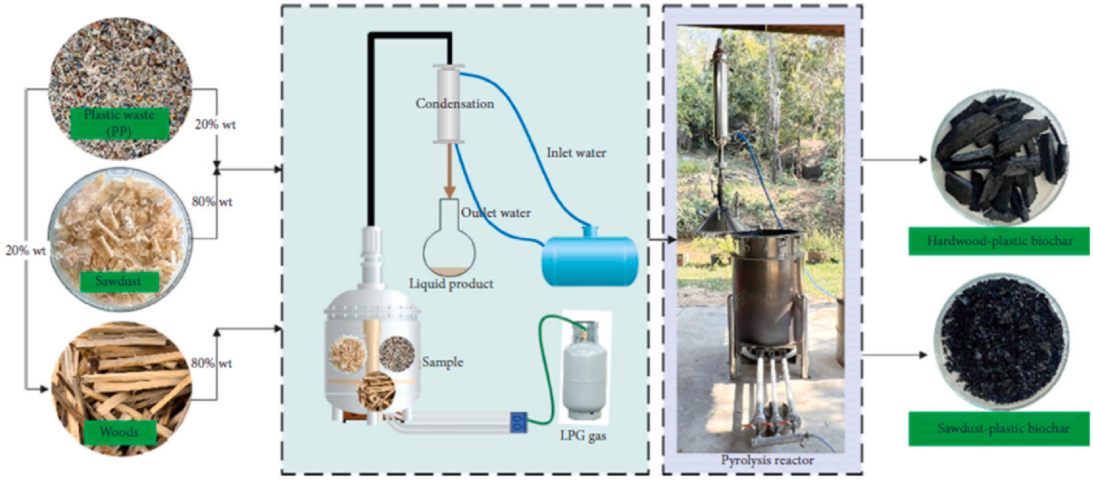


Fig. 3. Illustration of pyrolysis process for the production of hardwood–plastic and sawdust plastic biochars [87].

the plant source, fundamentally determines the yield, porosity, and graphitic-domain structure of the final carbon [21]. Lignin, a complex, amorphous polymer of phenylpropane units, is arguably the most valuable component for creating anode materials. Its high degree of aromaticity and thermal stability mean it resists depolymerization during pyrolysis, leading to a significantly higher char yield (40–50 wt%) compared to other components [22]. This aromatic network acts as a rigid scaffold, cross-linking upon carbonization to form the disordered, hard carbon structure that is ideal for hosting Li-ions. lignocelluloses have different compositions and are made up of highly interwoven elements that are chemically connected by covalent or non-covalent bonds [21]. Cellulose, a linear, crystalline polymer of glucose, behaves differently. Its ordered structure can, under specific high-temperature conditions, serve as a template for the formation of small graphitic domains (pseudo-graphitization) within the carbon matrix (Figs. 2–5) [23]. However, it is more prone to thermal decomposition than lignin, resulting in a lower char yield. Hemicellulose is the least thermally stable component. This amorphous, branched polymer decomposes at the lowest temperatures (220–315 °C), primarily volatilizing to produce light gases and tars [24].

A wide array of biomass sources has been investigated in previous study for carbon production, both individually or in co-pyrolysis with plastics. These sources are broadly categorized based on their origin and availability: Agricultural Residues: These are abundant and often underutilized, making them prime candidates for biochar production. Commonly studied examples include rice husk [25–27], wheat straw [28], corn stover [29,30], sugarcane bagasse [31], and miscanthus [32,33]. Forestry Waste: This category encompasses residues from wood processing and forestry operations. Examples include pinewood [34–36], bamboo [37], rubber wood sawdust [38], birch wood [39], sal wood sawdust [40]. Other common biomass are food waste [41,42], municipal sewage sludge [43] and macroalgae [44,45]. Therefore, the ideal biomass feedstock is not merely "any" waste, but one with a composition typically high lignin content that is predisposed to forming a high-yield, robustly porous, and disordered carbon framework. This is illustrated in Table 1, which compares the lignocellulosic makeup of common waste streams.

2.2. Plastic feedstocks

While biomass provides the structural foundation, plastic waste offers a powerful set of chemical functionalities. On their own, most plastics are poor precursors for carbon materials. Aliphatic polymers like polyethylene (PE) and polypropylene (PP), for instance, have a low carbon content and tend to depolymerize into volatile hydrocarbon monomers at pyrolysis temperatures, resulting in a near-zero char yield [58]. However, it is precisely this high volatile-matter content that makes them excellent additives to biomass. Conversely, other plastics

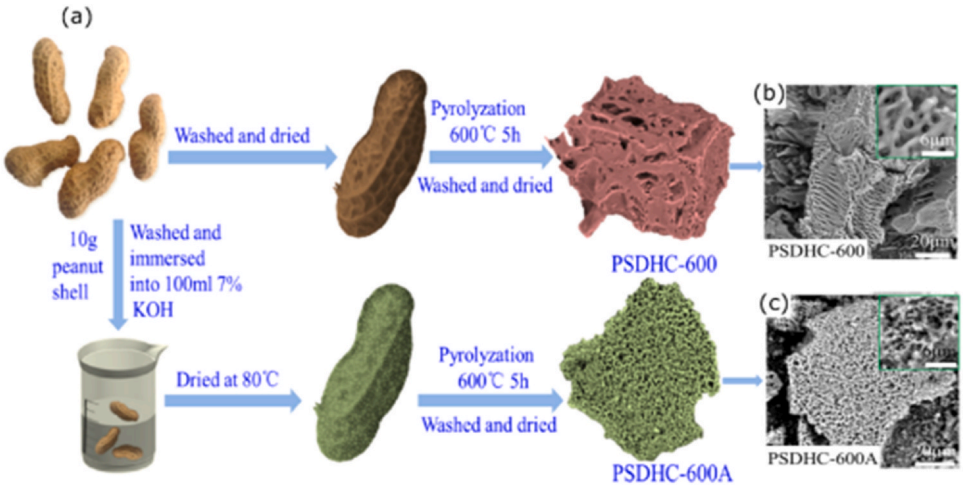


Fig. 4. (a) Effect of the chemical treatment on the AC properties, (b,c) SEM images of the peanut shell derived hard carbon and chemically activated peanut shell derived hard carbon. [101].

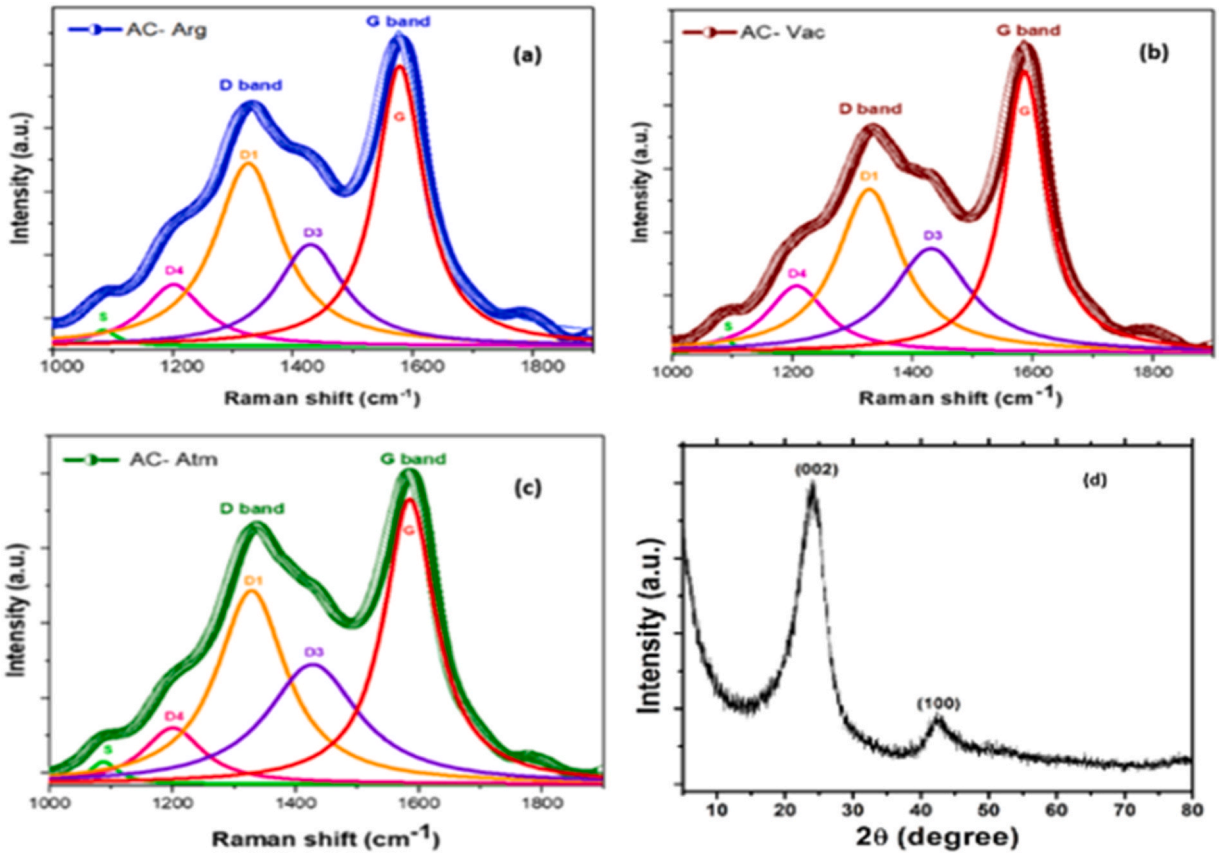


Fig. 5. (a) Fitted Raman spectra of olive pomace AC-Argon, (b) olive pomace AC-Vacuum, and (c) olive pomace AC-Atmosphere [109] (d) XRD pattern of rice husk [108].

offer intrinsic structural or chemical advantages. Poly (ethylene terephthalate) (PET), mainly found in beverage bottles, possesses aromatic rings in its backbone. These rings can contribute to the aromatic carbon framework, while its high oxygen content (approx. 33 % by mass) can facilitate O-doping of the final carbon, creating surface functional groups that enhance wettability and provide active sites for Li-ion storage [59]. Poly (vinyl chloride) (PVC), while environmentally problematic, has been explored as a carbon precursor that simultaneously acts as an activating agent [60]. Its thermal decomposition releases HCl, which can chemically etch the carbon, creating a high surface area. However, the extreme corrosivity of HCl and the potential for toxic dioxin formation present significant, and perhaps prohibitive, engineering and environmental challenges.

2.3. Co-carbonization of biomass and plastics feedstock

One of the advanced feedstock strategies involve the co-carbonization of biomass and plastic blends, a process that aims to capture the

Table 1
Lignocellulosic properties of some biomass wastes.

Lignocellulosic materials	Hemicellulose (%)	Cellulose (%)	Lignin (%)	References
Jungle cork tree	23.56	41.60	10.81	[46]
Abel. Shell (*Camellia oleifera*) (sclerenchyma cells)	50.4	17.6	30.9	[47]
Abel. Shell (*Camellia oleifera)* (parenchyma cells)	35.2	23.7	35.0	[47]
Onion skin	20–25	30–35	10–12	[48]
Banana peel	15–20	20–25	10–15	[49]
Bagasse	25–30	40–45	18–24	[50]
Pine Wood (Sawdust)	21.5	45.2	28.6	[51]
Rice Husk	24.5	38.2	15.8	[52]
Sugarcane Bagasse	23–32	38–50	18–26	[53]
Scot Pines (pine needles)	16.0 ± 0.6	23.5 ± 0.5	33.0 ± 2.0	[54]
Sal wood	14.59	52.36	11.18	[40]
Hardwood stems	24–40	40–50	18–25	[55]
Wheat Straw	28.0	40.5	18.2	[56]
Neem seed	14.36 ± 2.48	29.52 ± 0.42	5.96 ± 0.5	[57]
Pine cone	37.6	32.7	24.9	[34]

synergistic benefits of both materials. which is required for increasing the yield of the resulting materials. It can also improve the Specific surface area (SSA), aromaticity, and hydrophobicity of the biochar [61]. The interactions during co-pyrolysis are complex but can be broadly categorized into reasons such as, enhanced carbon yield which is the most significant synergy is the ability of plastics to boost the carbon yield of biomass [62]. During pyrolysis, molten PE or PP can act as a hydrogen-donor, transferring hydrogen radicals to the biomass-derived radicals. This introduction of reactive sites prevents them from forming light volatiles and instead promotes their recombination into a more stable, higher-mass solid char [63]. Secondly, the volatiles released from plastic decomposition (e.g., CH_4, H_2, CO) act as physical activators, etching the rigid biomass-derived char [64]. This synergy can create a well-developed hierarchical pore structure micropores for Li-ion storage and mesopores for electrolyte transport which can aid activation process. Lastly, the molten phase of plastics like PET can act as a solvent or wetting agent, intimately mixing with the biomass particles [65]. This ensures a homogeneous distribution of carbon, leading to a more uniform final material and efficient oxygen doping from the PET's ester groups [66].

3. Analysis of blending effects

The biomass-plastic blending ratio is a critical determinant of the resulting carbon's physicochemical properties, including SSA, porosity, functional groups, and carbon content, as well as the overall biochar yield [67]. Experimental findings consistently demonstrate that varying the mixing ratio can significantly alter the characteristics of the produced biochar [13]. This hybrid precursor approach produces more biochar than the biomass only does because of the influence of the plastics in during the co-carbonisation procedure [68]. For the case of biochar yield as seen in previous studies by comparing the different product yields, the experimental yields from the co-carbonisation vary depending on the type of precursor and the parameters selected, such as temperature, blending ratio, and residence time [13]. For instance, increasing the PET blending ratio with biomass can lead to an increase in the biochar SSA and enhance its adsorption properties. Gale et al. [69] studied, the addition of polystyrene (PS) or PET to corn stover (mass ratio 1: 1) and determined that there was improvement in the formation of biochar product with higher average pore size in the case of PS and higher SSA in the case of PET when compared to the control sample. However, the impact is not uniformly positive across all plastic types, blend ratio or conditions. For example, a drastic reduction in SSA was observed when a high proportion (50 wt%) of high-density polyethylene (HDPE) was added to rice husk during pyrolysis at 400 °C, likely due to the melting of HDPE covering and blocking existing pores and also the yield decreases for 41 wt% to 33 wt% as a result of HDPE mass ratio increase from 10 wt% to 30 wt%, However, further increasing the HDPE fraction to 40 % and 50 % increased yields at 400°C, potentially due to incomplete degradation of HDPE at this lower temperature [70]. Conversely, at higher temperature at about 500 °C, while a slight reduction in SSA was noted for low HDPE blends, an increase in yield, pore volume and size were observed, attributed to the release of volatiles from HDPE via thermal decomposition.

Recent evidence from a study by Mishra [46] on Jungle Cork Tree and varying ratio of non-recyclable PET (NRPET) showed that blending NRPET at 30 %, 50 %, and 80 % decreases the biochar yield as the blend ratio increases and ash content increases as blend ratio increases.

Some studies report positive synergy (higher char yield), while others report negative synergy (lower yield) using similar feedstocks [44]. This discrepancy does not imply that the results are incorrect, but rather that the outcomes are governed by subtle, often unreported, variables. A critical analysis suggests these contradictions arise from three primary factors namely.

Process Parameters like heating rate and reactor type are dominant. A slow pyrolysis process with a long gas residence time allows for extensive interaction between plastic-derived volatiles and the biomass char, promoting hydrogen transfer and maximizing synergistic char yield [71]. Conversely, a fast pyrolysis process can rapidly remove volatiles, minimising these interactions and favouring pore generation over yield. Many studies fail to adequately control or report these parameters, making direct comparisons difficult. Secondly, the degree of feedstock intimacy is crucial. A simple physical mixture of biomass powder and plastic pellets will pyrolyze semi-independently, limiting interaction. In contrast, methods that achieve intimate mixing, such as solvent-blending or high-shear melt-mixing, create a true composite where molten plastic can encapsulate the biomass, maximizing surface contact and synergistic reactions [72]. Finally, the catalytic role of inorganics (ash) in the biomass is a major confounding variable. Rice husk, for example, is rich in silica [52]. This silica can act as a catalyst, cracking the plastic polymers at lower temperatures than expected, which can lead to a negative synergistic effect on char yield as more material is converted to gas [73]. A study using high-purity pine wood (low ash) will therefore yield a fundamentally different synergistic outcome than one using high-ash rice husks, even with the same plastic.

Therefore, the challenge for the field is to move beyond mix-and-pyrolyze trials and toward a more predictive, mechanistic understanding. Future research must meticulously characterize the feedstock (including ash content), control and report the thermal process parameters, and consider the chemical-specific interactions (hydrogen-donation from PE vs. O-doping from PET) to truly harness the potential of these blended waste streams. Table 2 shows the summary of some

Table 2
Summary of Carbon Yields from Biomass-Plastic Co-carbonisation.

Feedstock Blend	Ratio (wt%)	Pyrolysis Temp. (°C)	Carbon Yield (wt%)	Key Finding / Synergistic Effect	Reference
Jungle cork tree and Polyethylene (PET)	70:30, 50:50, 20:80	500	24.71, 20.91, 17.51	Reduced char yield but improved the properties of the char, such as carbon content, heating value, bulk density, and electrical conductivity. Also, blending process led to a significant reduction in the oxygen content and surface area of the char	[46]
Pine wood and Polyethylene (PE)	50:50	500	32.5	Enhanced carbon yield due to plastic-derived hydrogen donation, reducing biomass decomposition volatiles	[73]
Rice husk and Polypropylene (PP)	70:30		28.4	Synergistic increase in fixed carbon content; plastic promotes aromatization of char.	[67]
Corn stover and Polystyrene (PS)	60:40	550	35.2	Improved char porosity and yield via radical interactions; reduced bio-oil acidity	[74]
Sugarcane bagasse and Low-density PE (LDPE)	80:20	450	29.8	Synergy in thermal stability, leading to higher carbon retention and lower ash content.	[75]

selected biomass/plastic carbon yields for biomass-plastic co-carbonisation, illustrating the variability based on feedstock, ratio, and treatment condition.

4. Synthesis and activation method

The synthesis of derived-carbon from biomass and plastic need to initially undergo thermochemical conversion. Various thermochemical techniques have been studied to produce char from biomass and plastic. The most commonly and effective techniques is the slow pyrolysis (used interchangeably with carbonisation) and hydrothermal carbonisation [13]. Other thermochemical method that has been used include gasification and torrefaction [76]. The temperature, heating rate, and atmosphere during carbonisation critically affect the degree of graphitization, defect density, and microstructure of waste-derived carbons [77–79]. Higher temperatures generally increase graphitization but may reduce porosity and functional group content [49,77,80]. Also, these parameters, in turn, govern the material's electrochemical behaviour, including its Li-ion storage capacity, rate capability, and ICE [81].

4.1. Carbonisation/pyrolysis

The process of carbonisation converts the precursor into a solid, carbon-rich char. This process, conducted in an inert atmosphere, involves a series of complex decomposition and recombination reactions. The most influential parameter in this stage is the final treatment temperature, which acts as a lever to balance two competing sets of properties: heteroatom retention/defect density versus electronic conductivity [8,66].

4.1.1. Low-temperature carbonization (400–700 °C)

Pyrolysis at these relatively low temperatures yields a char that is highly disordered and rich in non-carbon elements (O, N, H) from the original feedstock [82]. This heteroatom-rich matrix possesses an extremely high density of structural defects. These sites are not flaws; they are electrochemically active centres for Li-ion storage, contributing significant capacity in the sloping voltage region (0.1–1.5 V) and enhancing surface wettability [83]. The primary drawback, however, is poor electronic conductivity, as the carbon matrix lacks significant sp^2-hybridized graphitic domains, which fatally compromises rate performance [24,84].

4.1.2. High-temperature carbonization (800–1200 °C and above)

As the temperature increases, a profound structural re-ordering occurs. Heteroatoms are volatilized (e.g., CO, H_2, N_2), and the carbon atoms begin to self-assemble into small, stacked graphitic microdomains (pseudo-graphitization). This process, tracked by the decreasing d_{002}-spacing in XRD and a sharpening G-band in Raman spectroscopy, drastically improves the material's electronic conductivity [85]. However, this result comes at a steep cost: the loss of heteroatoms and the repair of defects eliminate many of the high-energy Li-ion storage sites. This results in a lower reversible capacity, even as the rate capability improves [86].

Therefore, the choice of carbonisation temperature is a critical trade-off. It is a decision between a high-capacity, defect-rich material with poor kinetics (low temp) and a high-conductivity, more graphitic material with lower capacity (high temp). The challenge for the field is to find an optimal balance, or to develop multi-stage processes that can decouple these properties.

4.2. Activation methods

The raw char produced by pyrolysis is often dense, with a low SSA and inaccessible pores. To create the high-surface-area, porous network essential for electrolyte-ion transport and surface-based Li-ion storage,

a secondary activation step is required [88]. This is broadly achieved via two pathways: physical activation and chemical activation.

4.2.1. Physical activation

Physical activation is a gas-phase etching process, typically conducted at high temperatures (700–1000 ˚C) using oxidizing agents like steam (H_2O, carbon dioxide (CO_2), or air. The process is a controlled gasification, where the agent selectively reacts with the most reactive carbon atoms (amorphous regions, defect sites) to form volatile products, leaving pores behind [79,89,90]. This method is often preferred for its relative simplicity and lower environmental footprint, as it avoids corrosive liquid chemicals and simplifies product workup (no extensive washing). The resulting carbons are typically microporous (< 2 nm) [25]. However, physical activation is often slower, more energy-intensive (due to higher temperatures), and generally produces materials with a lower SSA and less pore-volume diversity compared to its chemical counterpart [91,92].

4.2.2. Chemical activation

Chemical activation is usually performed either as a single-step or a two-step process [93]. In the single-step approach, biomass precursors are first impregnated with an activating agent and then heated in an inert atmosphere at temperatures between 450 ℃ and 900 ℃ to produce activated carbon. In the two-step method, the biomass is initially carbonized at 400–450 ℃, after which the pre-carbonized material is mixed with chemical activators and further heated in an inert atmosphere at 650–900 ℃. The activating agent simultaneously dehydrates, cross-links, and chemically etches the carbon structure. The choice of activating agent strongly influences the activation mechanism and determines how pore structures and surface area are developed [25]. Alkaline compounds such as NaOH and KOH [91,94], acidic chemicals (phosphoric acid (H_3PO_4) [95] or Hydrochloric acid (HCl) [96], sulfuric acid (H_2SO_2), nitric acid (HNO_3), and salts (potassium carbonate (K_2CO_3), zinc chloride ($ZnCl_2$) and ferric salt chlorides), have been used for biochar activation [81,97]. Potassium hydroxide (KOH) is the most powerful and widely studied chemical activator. Its mechanism, is a complex and aggressive multi-step process [89]: At lower temperatures (< 400 ˚C), KOH acts as a strong dehydrating agent [94]. Above 400 ˚C, KOH reacts with carbon, reducing to metallic potassium [91]. The vaporization and subsequent removal of this intercalated potassium metal (via washing) leaves behind a well-developed, interconnected network of micropores and mesopores, resulting in an ultra-high SSA. Other common agents include zinc chloride ($ZnCl_2$) and phosphoric acid (H_3PO_4). $ZnCl_2$ acts as a strong dehydrating agent and a Lewis acid. During pyrolysis, the molten $ZnCl_2$ functions as a template into which the carbon structure forms. Upon washing with acid to remove the zinc salts, a highly porous, typically mesoporous, structure is left behind [98]. Its primary drawback is the environmental toxicity of zinc compounds and the need for stringent recovery. H_3PO_4 is also a dehydrating agent and a catalyst. It cross-links the lignocellulosic polymers via phosphate ester bridges. Upon heating, the H_3PO_4 and its derivatives (P_2O_5) expand, acting as a template to the carbon structure. This process not only creates porosity but also results in phosphorus doping, which is highly beneficial for electrochemical performance [99,100].

4.3. Heteroatom doping strategies

The intentional introduction of heteroatoms (such as N, P, S, B) to replace carbon atoms in the sp^2 lattice is a proven strategy to enhance electrochemical performance. Doping can (1) improve electronic conductivity, (2) create new extrinsic defects that act as active sites for Li-ion storage, and (3) enhance the surface affinity for the electrolyte [83,102]. In situ doping is the most economical and scalable method. It relies on using precursors that are naturally rich in the desired heteroatom. This is where feedstocks like N-rich food wastes (such as chitosan from shrimp shells) or O-rich PET are used [102]. The co-pyrolysis of biomass with N-rich plastics or polymers (melamine, polyacrylonitrile) is also a powerful in situ strategy. On the other hand, post doping strategy synthesized carbon is subjected to a secondary high-temperature treatment in the presence of a doping-agent. While this approach offers more precise control over the doping level, it adds significant cost, complexity, and energy consumption to the overall process [103].

5. Key properties of biomass derived activated carbon anodes

5.1. Porosity and surface area

The porous structure of anode materials is arguably its most critical property for electrochemical performance, as it directly dictates the available SSA for ion storage and the pathways for electrolyte diffusion [90]. The pore network is typically classified into three categories based on size: micropores (< 2 nm), mesopores (2–50 nm), and macropores (> 50 nm). A hierarchical pore structure, featuring a combination of these pore types, is considered ideal. Micropores act as primary storage sites for lithium ions, particularly for hard carbons where ions are stored in nanopores and at defects [104]. Mesopores provide efficient and rapid diffusion pathways for the electrolyte, reducing internal resistance and enhancing rate capability [105]. Macropores function as reservoirs, ensuring a constant and ample supply of electrolyte to the electrode surface [106]. A study by Zheng et al. [80] on duckweed emphasized the importance of a balanced hierarchical pore structure, noting that the combination of micropores and mesopores minimizes the formation of an excessive solid electrolyte interphase (SEI) layer. There is a common misconception, often translated from supercapacitor research, is that a higher SSA is an unqualified-for-good. For LIB anodes, this is a critical error. The vast, high-energy surface of an activated carbon (e.g., > 1000 m^2/g) is not inert; it is a massive, reactive interface. Upon the first charge, this surface draws Li^+ from the electrolyte to form a passivating layer known as the Solid Electrolyte Interphase (SEI). An excessively high SSA leads to the formation of a thick, non-uniform SEI, which irreversibly consumes a large quantity of lithium ions [107]. This manifests as the single greatest challenge for these materials - a disastrously low ICE. An anode with a 50 % ICE, for example, consumes half the battery's active lithium on the first cycle, rendering it commercially non-viable. For instance, Ahmed et al. [108] reported AC from rice husk activated with KOH reached an SSA of 1962.32 m^2/g, delivering discharge capacity of 321 mAh/g at 100 mA/g and retained capacity of about 250 mAh/g and a coulombic efficiency of 92 % after 400 cycles. In contrast, plastic-derived carbons often have lower SSA but a more developed mesoporous structure due to the nature of their polymer chains and the release of volatiles during pyrolysis. The quality of the surface, defined by its engineered pore hierarchy and chemical properties, is therefore more critical than simply maximizing its quantity.

5.2. Graphitization and defect density (XRD, raman)

Beyond the pore structure, the atomic arrangement of the carbon lattice itself is a primary determinant of performance. This is probed using X-ray Diffraction (XRD) and Raman spectroscopy. X-ray Diffraction (XRD) provides a view of the long-range order. A typical hard carbon XRD pattern shows two broad, low-intensity peaks at approx. 23–25^0 and approx. 43^0, corresponding to the (002) and (100) planes. The position of the (002) peak is used to calculate the average interlayer spacing (d_{002}). Unlike graphite (d_{002} approx. 0.335 nm), waste-derived hard carbons have an expanded and disordered spacing (d_{002} > 0.35 nm), which is essential for accommodating Li-ions. Furthermore, the breadth of these peaks can be used in the Debye-Scherrer equation to estimate the size of the graphitic microdomains (L_a, L_c).

$$L = \frac{K\lambda}{\beta \cos\theta}$$

where K is the shape factor, λ is the X-ray wavelength, β is the full-width-at-half-maximum of the peak, and θ is the Bragg angle.

Raman Spectroscopy is arguably the most powerful tool for probing short-range disorder in carbon [24,84]. The Raman spectrum is dominated by two features: the D-band (approx. 1350 cm^{-1}), which is activated by sp^3 defects, edges, and disordered lattices, and the G-band (approx. 1580 cm^{-1}), which represents the in-plane bond-stretching of sp^2 hybridized carbons in the graphitic lattice. The intensity ratio of these peaks (I_D / I_G) is a direct, quantitative measure of the material's defectiveness [109]. In conventional graphite research, a high I_D / I_G ratio is undesirable, indicating a damaged crystal. In hard carbon anodes, the opposite is the case - a high I_D / I_G ratio signifies a high density of defects, which act as high-energy, active storage sites for Li-ions, contributing directly to the high sloping capacity [49].

5.3. Surface chemistry and doping

The surface chemistry of activated carbons, particularly the presence of heteroatoms and functional groups, significantly influences Li-ion adsorption and the formation of the SEI layer [107]. X-ray Photoelectron Spectroscopy (XPS) is essential for quantifying the elemental composition and, more importantly, the chemical bonding states on the material's surface. For heteroatom-doped carbons (such as, N, O, P, S). For example, a high-resolution scan of the N 1 s peak can be deconvoluted to identify and quantify the specific bonding configurations: Pyridinic-N (at sp^2 carbon edges), (substitutional within the sp^2 lattice). This distinction is critical. Graphitic-N tends to enhance electronic conductivity, while pyridinic-N and pyrrolic-N, which are often co-located with carbon vacancies, create a high density of electrochemically active sites for Li-ion binding, thus boosting storage capacity [110]. Fourier-Transform Infrared Spectroscopy (FTIR) complements this by identifying bulk functional groups (C═O, C-O-C, -OH) remaining from the precursor, which can also act as active sites and improve the electrode's wettability by the polar electrolyte. Available research indicates that many biomasses naturally contain nitrogen functionalities, allowing for self-doping during preparation. Heteroatom doping is a multi-modal performance enhancer that improves not only capacity but also conductivity and structural stability [83]. For instance, nitrogen doping in oil palm empty fruit bunch carbon significantly improved its discharge capacity and coulombic efficiency [86]. Similarly, phosphorus doping of waste PET-derived hard carbon enhanced its electrical conductivity and structural stability [111]. Also, doped biomass from persimmon branches with nitrogen using urea to improve its pore structure utilisation efficiency. It was reported for 4.66 % nitrogen doping level exhibited the more pore utilisation, thereby resulting to 92 % capacity retention after 8000 cycles, showing good cycling stability [112]. These heteroatoms alter the electronic structure of the carbon framework, creating more active sites for Li-ion adsorption and expanding the carbon lattice spacing [113], which facilitates Li-ion diffusion and reduces internal resistance. This demonstrates that doping is not a simple additive process but a foundational strategy for modifying the core physicochemical properties of the material itself. Performance of derived carbon material for anode in lithium-ion can only be understood by explicitly linking synthesis, properties, and electrochemistry. The literature is a minefield of seemingly contradictory reports, where one study claims a material is superior based on high capacity, while another dismisses a similar material due to low ICE. Table 3 provides a critical, comparative summary of representative data from recent studies. This synthesis-to-performance map allows us to identify the field's most important trade-offs.

A critical analysis of information in Table 3 and supporting literature reveals several key trends and some contradictions in how synthesis strategies and material properties affect electrochemical

Table 3
Correlation of Synthesis, Properties, and Electrochemical Performance of Activated Waste-Derived Carbon.

Feedstocks (blend)	Activation Synthesis	Key Properties	Electrochemical Metrics	Test Conditions	References
Waste tea leaves	$KHCO_3$ activation + pyrolysis @ 700 °C at a rate of 5 °C min^{-1} for 2 h	High surface area, large layer spacing, micro/mesopores	553 mAh/g, stable over 2000 cycles	Coin cell, 0.1 A/g, @ RT	[114]
Birch tree waste + SnO_2	H_3PO_4 activation, pyrolysis, SnO_2 composite	Macroporous, Sn-doped, defect-rich	319–453 mAh/g (120 cycles), high rate performance	Li metal half-cell, 1 C/0.1 C, @ RT	[115]
Polypropylene plastic waste	Microwave-assisted pyrolysis, HNO. activation	3D porous, mesoporous, well-organized structure	381 mAh/g (initial), 355 mAh/g (0.2 A/g,100 cycles)	Coin cell, 0.2 A/g, 230°C,25 min	[65]
Furfural biorefinery bagasse	Pyrolysis (700°C), KOH/steam activation	405.8 m^2/g, hierarchical pores, oxygen-rich, amorphous	1055 mAh/g (initial), ~ 250 mAh/g (100cycles)	Half-cell, C/2rate, 0.01–3 V, @ RT	[116]
Rice husk	KOH activation (850°C for 1 h)	Spherical, 40–90 nm, amorphous, high defect density	321 mAh/g (1st),253 mAh/g (400cycles), 81 %retention	Coin cell, 100 mA/g, 0–2.5 V, room temp	[117]
Banana peel waste	One-step activation / carbonization (H_3PO_4, KOH, $ZnCl_2$)	815 m^2/g (H_3PO_4), microporous, good conductivity	272 mAh/g (0.2 C, 200cycles), high-rate capability	Coin cell,0.2 C, 0.01–3 V, room temp	[49]
PET bottles	Ionothermal synthesis (CU-DES), annealing / pyrolysis	Low surface area, high graphitization, N-doped	460 mAh/g (100 mA/g), 98 %retention (100cycles)	Coin cell, 100 mA/g, 0.01–2.8 V, 25°C	[66]
Spartina alterniflora	NaOH activation, N-doping (melamine)	Amorphous, porous, N-doped (SANC: 780.8 mAh/g)	456.7–780.8 mAh/g, 412.9 mAh/g (600cycles, SANC)	Coin cell, 6 mA/g, 600cycles	[118]
Lignin (N,P-co doped)	g-C_3N_4 template, lecithin P-source, annealing	675.4 m^2/g, mesoporous, high defect, N,P-doped	1264.3 mAh/g (100 mA/g),1463.8 mAh/g (1 A, 500 cycles)	Coin cell, 100 mA/g, 0.1–3 V	[119]

performance. For example, $KHCO_3$ activated tea leaf carbon and KOH/steam-activated bagasse both show high initial capacities due to their micro/mesoporous structures and large surface areas. However, excessive disorder and high surface area can lead to rapid capacity fading, as seen in the bagasse-derived carbon, where initial capacity is high but retention drops significantly over cycles due to unstable SEI and lithium trapping. The birch/SnO_2 composite out performs bare carbon due to improved electron transport and additional lithium storage mechanisms [115]. Hierarchical porosity supports both high capacity and stable SEI formation, minimizing irreversible capacity loss and improving long-term cycling, as demonstrated by nutmeg shell-derived carbon. While high surface area and porosity boost initial capacity, they can also promote excessive SEI formation and capacity fading, as seen in bagasse and some highly activated carbons. In contrast, denser, more ordered carbons was achieved in PET (using choline chloride deep eutectic salts through ionothermal synthesis) shows lower initial capacity but superior retention [66]. N-doping in PET-derived carbon increases active sites and initial capacity, but too much disorder can reduce coulombic efficiency and cycling stability [120,121].

A hybrid approach combining moderate chemical activation, controlled graphitization, and judicious heteroatom doping or composite formation appears most promising. Specifically using of chemical activation at optimized temperatures to balance surface area and pore structure or incorporation of conductive additives or mild graphitization to stabilize the structure and SEI [120]. Limited targeted doping or composite formation to further boost performance without sacrificing stability. It is also important to note that while high SSA and porosity boost initial capacity, they can also promote excessive SEI formation and capacity fading. Also, N-doping can enhance capacity and rate performance, but excessive doping or disorder may harm voltage efficiency and cycling stability. Lastly, Metal oxide composites improve performance but add complexity and may introduce new degradation mechanisms if not well integrated [115].

6. Electrochemical performance in LIBs

6.1. Li-ion storage mechanisms

The charge storage mechanism in derived carbons, particularly hard carbons derived from biomass and plastics, is distinct from the pure intercalation mechanism of graphite [85,122]. It is a dual-storage process comprising two regions in the charge-discharge profile. The first is a sloping region (1.5 V to 0.1 V vs. Li^+/Li) which is the signature of hard carbon and the primary source of its capacity. This region is not intercalation. It is a faradaic, pseudocapacitive process representing the binding of Li-ions to a high density of active sites, including surface functional groups (such as C═O, C-O-C) and structural defects [123,124]. The more defects and heteroatoms a material possesses, the more pronounced this sloping region becomes. The second is a low-voltage plateau region, typically below 0.1 V, this region is analogous to, but distinct from, graphite. It represents the intercalation of Li-ions between the disordered, non-parallel graphitic microdomains identified by XRD. The expanded d_{002} spacing of hard carbon is critical, as it provides a low-energy barrier for Li^+ insertion [125]. The low-voltage end (around 0.01 V)and the precise mechanism of this end is still debated but is widely attributed to Li-ion storage in micropores (pore-filling) or the formation of Li quasi-metallic clusters within closed-pore structures [125]. Muruganantham et al. [126] reported a study on mango-peel-derived activated carbon carbonated at 1000℃ exhibits a hybrid storage mechanism combining adsorption on defect sites and pores, and intercalation into graphitic layers. The Cyclic voltammetry (CV) shows a broad cathodic peak at ~0.8 V in the first cycle due to solid electrolyte interphase (SEI) formation, with overlapping subsequent cycles indicating stability. This illustration can be seen in Fig. 6, including a comparison carbonisation at 600℃ for the same biomass precursor. Also, the profiles of the Galvanostatic charge-discharge (GCD) reveal a sloping region (> 0.1 V) attributed to capacitive Li^+ adsorption and a plateau (< 0.1 V) from intercalation. The relative contribution of each mechanism depends on the material's microstructure, which is dictated by the synthesis and activation conditions [127]. This multi-site storage mechanism, is the fundamental reason waste-derived carbons can outperform graphite. They store lithium not only between their carbon layers but also on their surfaces and at their defects.

6.2. Influence of heteroatoms and defects

Structural defects and the presence of heteroatoms are not merely incidental features; they are crucial for improving the electrochemical properties of waste-based carbon anodes [102,128,129]. Nitrogen doping is highly effective as identified by the role of graphitic-N, pyridinic-N and pyrrolic-N, they are co-located with carbon vacancies, which creates a high density of electrochemically active sites that strongly bind Li-ions, directly boosting the sloping capacity [130]. For Oxygen, it is often seen as an impurity, provides redox-active quinone (C═O) groups that undergo a reversible reaction with Li-ions. This is a fast, pseudocapacitive mechanism that adds to the sloping capacity and improves the electrode's wettability by polar electrolytes [131]. Lastly, doping with larger atoms like sulfur or phosphorus can expand the carbon lattice, further increasing the d_{002} spacing and reducing the energy barrier for intercalation, thereby enhancing diffusion kinetics. P-doping, often a byproduct of H_3PO_4 activation, can also create P-C and P-O-C bonds that improve charge transfer [132].

7. Key performance metrics and critical analysis

The literature is well established with materials boasting ultra-high capacities (> 800 mAh/g) that are rendered useless by catastrophic ICE. This is the field's central trade-off. However, recent work has demonstrated that by optimizing defect-density rather than maximizing surface area, a high capacity can be achieved without this fatal penalty. The optimum point involves creating a material rich in heteroatom defects but with a moderate, mesoporous SSA. Long-term stability is also a concern; the very defect sites that provide high capacity can be subject to structural fatigue or continuous electrolyte-side reactions, leading to capacity fade on an extended cycle.

7.1. Rate capability and diffusion kinetics

The true differentiator for advanced WDCs is their potential for superior rate capability. The mechanism of ion movement in a disordered carbon is fundamentally different from that in graphite [133]. To quantify this, cyclic voltammetry (CV) at various scan rates is used to probe the kinetics via the Dunn method. The b-value distinguishes between two storage types: A diffusion-controlled process (b = 0.5) occurs in solid-state intercalation in graphite, which is usually slow. The other is the capacitive-controlled process (b = 1.0) (e.g., surface adsorption, pseudocapacitance), which is considerably very fast. While graphite is almost purely diffusion-controlled, high-performance hard carbons show a dominant capacitive contribution (b > 0.8). This confirms that their high capacity is derived from fast, surface-based mechanisms at defects and in pores, not from slow intercalation. This high capacitive contribution is the physical reason for their superior rate performance [16]. Furthermore, techniques like the Galvanostatic Intermittent Titration Technique (GITT) and EIS can be used to calculate the Li-ion diffusion coefficient (D_{Li+}). In many WDCs, the D_{Li+} is found to be 1–2 orders of magnitude higher than in graphite [6]. This is because the Li-ions do not need to be formally de-solvated and squeezed into a tight crystal lattice; rather, they can move rapidly through the more open, ion-permeable mesoporous channels. Table 4 provides a summary of key performance metrics from selected studies.

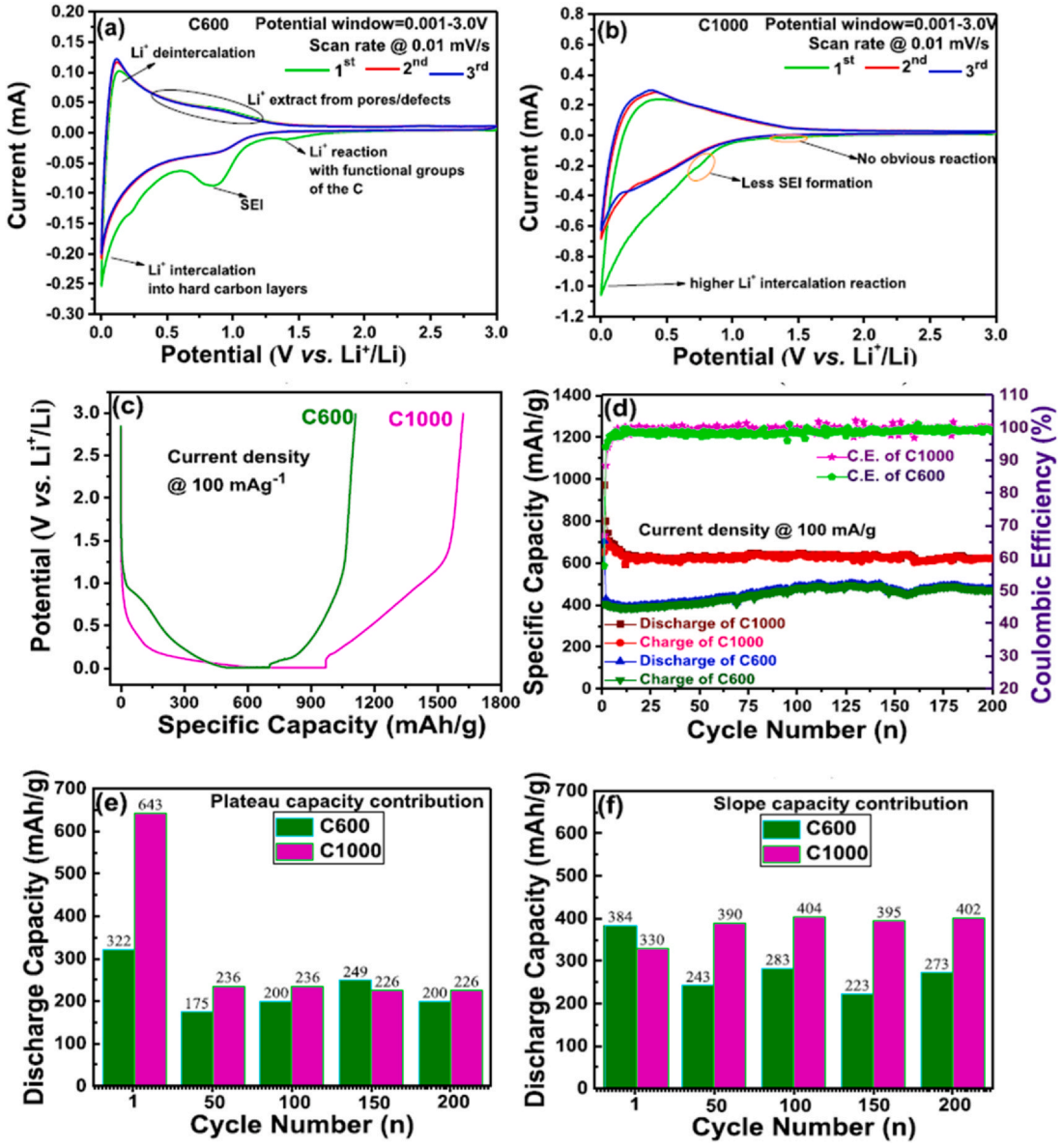


Fig. 6. Electrochemical behaviour of mango peel-derived carbons at 600 °C (C600) and 1000 °C (C1000) in lithium-ion cells: (a,b) CV curves at 0.01 mV s^{-1} , (c) initial charge–discharge profile at 100 mA g^{-1} , (d) cycling stability, and (e,f) plateau and slope capacity contributions [126].

8. Waste-derived carbon composites and new emerging materials

ICE and high capacity are not the only trade-offs in the performance and sustainability of WDC, the challenges of long-term cycling stability under high mass loading still persist. To circumvent these limitations, the research frontier has decisively moved toward the development of advanced composites. This approach treats the porous WDC not as the sole active material, but as a multifunctional conductive scaffold, a

Table 4
Electrochemical evaluation of Waste-Derived Carbon Anodes for Lithium-Ion Batteries.

Feedstocks	Rate Capacity (mA/g)	Initial Coulombic Efficiency (%)	Capacity (mAh/g)	Capacity Retention (%)	Test Conditions (Coin Cell)	Refs
Tea leaves	100	68.2	553	95 (2000cycles)	0.1 A/g, RT	[134]
Birch/SnO_2	100/1000	70.1	319–453	90 (120cycles)	1 C/0.1 C, RT	[135]
Waste tires	50	65.3	880	80 (100cycles)	50 mA/g, RT	[136]
Polypropylene	200	72.5	381(initial)	93 (100cycles)	0.2 A/g, 230°C, 25 min	[137]
Bagasse	100	61.2	1055(initial)	24 (100cycles)	C/2, 0.01–3 V, RT	[138]
PET bottles	100	75.0	460	98 (100cycles)	100 mA/g,0.01–2.8 V,25°C	[139]
Garlic stem	100	70.0	480	90 (3000cycles)	Not specified	[140]
Packing peanuts (Plastic)	100/1000	76.5	420 (0.1 C), 220 (1 C)	100 (100cycles)	0.1 C/1 C, RT	[141]
Spruce tree	100, 500, 1000	91.1	370, 332.4, 319	98.50 (5000cycles)		[142]

RT = Room Temperature

volumetric buffer, and a porous ion-highway that can host and stabilize other, ultra-high-capacity materials.

8.1. Metal oxide hybrids

Transition metal oxides (TMOs) have been investigated in several studies as anodes due to their staggering theoretical capacities [143], which actually exceed that of graphite. Their storage mechanism, however, is based on conversion ($Fe_2O_3 + 6Li^+ + 6e^- \rightarrow 2Fe^0 + 3Li_2O$) or **alloying** ($Sn + xLi^+ + xe^- \rightarrow Li_xSn$) reactions [144]. These reactions are plagued by two fatal flaws when TMOs are used in their bulk form. The insertion and extrusion of this many lithium ions induce massive volumetric expansion and contraction often 150–300 %, which pulverizes the particle and severs electrical contact. Most TMOs are poor electronic conductors, leading to high internal resistance and rapid capacity fade at high charge rates. This is where the synergy with WDCs becomes a powerful solution. By synthesizing a composite where TMO nanoparticles are embedded within the porous, conductive carbon matrix a robust, high-performance anode is created. The WDC matrix serves three simultaneous functions as conductive pathway, volumetric buffer and dual-storage component [145]. For example, encapsulating bimetallic sulfides (CoMoS) in a nitrogen-doped carbon shell derived from dopamine results in a high reversible capacity (709 mAh/g after 100 cycles at 200 mA/g) and excellent retention (94 % after 600 cycles) [138]. The carbon shell improves conductivity, buffers volume changes, and stabilizes the solid electrolyte interphase (SEI). Similarly, Sn-based and TiO_2-based hybrids benefit from the carbon matrix, which mitigates pulverization and aggregation, leading to improved rate capability and longer cycle life [146,147]. These hybrids consistently outperform pure waste-derived carbon anodes, which typically offer lower capacities (200–400 mAh/g) and less robust cycling.

8.2. Advanced hybrids with silicon (Si)

Silicon offers a theoretical capacity nearly ten times that of graphite, however, it represents an extreme case of the TMO problem, with volume changes exceeding 300 %. Recent work using natural diatomite as a template to create hierarchical silicon-carbon hybrids demonstrates that such structures can deliver high specific capacities (approx. 1153 mAh/g) and outstanding cycling stability in all-solid-state LIBs [148]. Two-dimensional covalent encapsulation of silicon with carbon further enhances mechanical integrity, rate capability, and interfacial stability, enabling high reversibility and capacity retention [149,150]. These silicon-carbon hybrids far exceed the performance of conventional waste-derived carbon anodes, especially in terms of capacity and cycle life.

8.3. Kinetic-enhancing hybrids

A different class of composite focuses not on boosting capacity, but on mastering kinetics. 2D materials like MXenes ($Ti_3C_2T_x$) are ideal partners for WDCs. MXenes are 2D flakes with metallic-level conductivity and highly functionalized, hydrophilic surfaces. When WDC particles are composited with MXene nanosheets, the synergy is purely kinetic. The 2D MXene sheets wrap the WDC particles, forming a continuous, low-resistance electron pathway, very similar to graphene-like network [151]. Also, the hydrophilic functional groups make the entire composite lithiophilic, improving electrolyte wettability and ensuring that Li-ions can rapidly access the WDC's micropores. When combined with nitrogen-doped graphene-like carbon, MXene-based hybrids achieve reversible capacities of 400 mAh/g higher than pure MXene and excellent cycling stability [147]. MXene also serves as a conductive binder for thick silicon anodes, enabling very high areal capacities (up to 23.3 $mAhcm^{-2}$) and robust mechanical properties [152]. A non-hazardous eutectic method of the synthesis of a simple hybrid of porous carbon from wood fiber and MXene is shown in Fig. 7. These hybrids address the sluggish kinetics and poor rate performance of traditional carbon anodes, offering both high capacity and fast charge/discharge capability. Table 5 shows comparison in performance of some Waste-Derived Carbon Composites and new emerging materials.

Hybridization of waste-derived carbon with metal oxides, silicon, or MXenes leads to substantial improvements in capacity, cycling stability, and rate performance compared to pure carbon anodes. Metal oxide and silicon hybrids particularly excel in capacity and stability, while MXene hybrids offer superior kinetics and enable thick, high-loading electrodes. These advances position hybrid waste-derived carbon materials as leading candidates for next-generation LIB anodes.

9. Research gaps and challenges

Despite the impressive progress, the path to commercialization is blocked by a series of well-defined, formidable challenges that the field must collectively address.

9.1. Low initial coulombic efficiency (ICE)

A low ICE is the single greatest technical flaw of most WDC materials. An ICE of 40–70 % is common for high-capacity, high-SSA materials, and this is commercially non-viable. This low efficiency stems from the irreversible consumption of lithium during the formation of the Solid Electrolyte Interphase (SEI) on the vast, defect-rich carbon surfaces. This is not a problem that can be ignored in pursuit of higher capacity.

9.2. Process scalability and techno-economics

Aggressive chemical activation produces corrosive, toxic, and expensive-to-recycle waste streams, negating the clean energy intention of the feedstock. Physical activation, while cleaner, is energy-intensive. Also, the inherent variability of waste precursors can lead to inconsistent material properties, these can be a major barrier to reliable large-scale manufacturing.

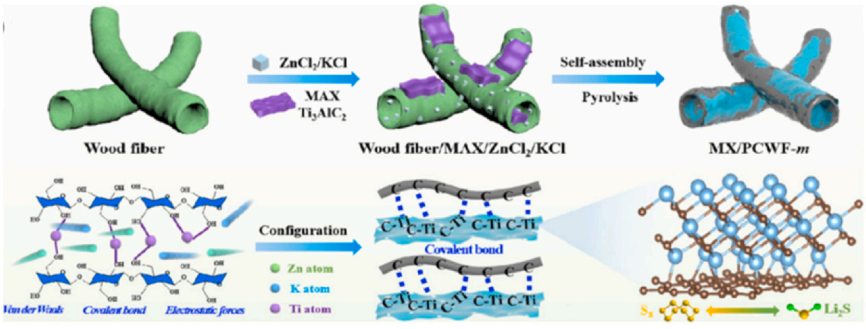


Fig. 7. Illustration of biomass derived porous activated carbon composite with MXene nanosheets using wood fiber [151].

Table 5
Comparative performance of hybrid type anode in lithium-ion batteries.

Anode material	Typical Capacity (mAh/g)	Cycle Stability (retention)	Rate Capability	Key Advantage over Pure Carbon	Citations
Metal Oxide/Carbon	400–900	85–95 % (100–600 cycles)	Good	Higher capacity, stability	[138,146]
Silicon/Carbon	700–1200	> 90 % (100–500 cycles)	Excellent	Ultra-high capacity, robust	[148–150]
MXene /Carbon	400 +	High (500 + cycles)	Excellent	Fast kinetics, thick electrodes	[147,152]
Waste-Derived Carbon	200– 400	80–95 % (100–900 cycles)	Moderate	Sustainable, low cost, lower ICE/capacity	[140]
Traditional Graphite	350–372	> 90 % (500 + cycles)	Moderate	Mature, stable, but limited capacity/rate	[17]

10. Future outlook

Addressing these challenges requires a paradigm shift away from regular mix-and-pyrolyze discovery and toward intelligent, targeted material and process design. Future research must focus on developing scalable, safe, and air-stable pre-lithiation methods tailored for high-SSA carbon anodes. The most direct way to solve the low ICE problem is introduce a sacrificial lithium source into the anode, which is consumed to form the SEI, leaving the cathode's lithium inventory intact. Secondly, the field has established the benefits of single-atom doping (N, P, S). The next frontier is multi-heteroatom co-doping (N/P, N/S, or even N/P/B). The synergistic effects of co-dopants, where one atom like Nitrogen creates active sites and another Phosphorous expands the lattice and improves conductivity may offer a new, high-dimensional space for tuning the electronic structure and defect chemistry to simultaneously optimize capacity and kinetics [112]. Thirdly, the future should shift to adopting Artificial Intelligence (AI) and Machine Learning (ML), this can help to improve on the slow and inefficient one-variable-at-a-time experimentation, the vast synthesis process and multivariate space (feedstock ratio, temperature, activation time, dopant concentration). Researchers can use ML models trained on the vast, existing literature data to predict how a given set of synthesis parameters will map to a desired set of electrochemical properties. This data-driven approach can rapidly screen thousands of virtual experiments, identify non-intuitive synergistic effects, and guide researchers to the most promising, high-performance materials, dramatically accelerating the discovery-to-deployment pipeline. Finally, the field must mature in its evaluation. Future work should be include demonstrating stable cycling in a full-cell, which is the only true measure of commercial viability. And providing at least a preliminary analysis of the proposed process's cost and environmental footprint compared to the commercial graphite baseline.

11. Conclusion

This review assessed the production and application of waste derived carbon for lithium-ion battery anodes. It established the importance of lithium-ion batteries in energy storage and the limitations of traditional graphite anodes. The various synthesis methods that have been used which influence surface area, pore structure, and conductivity of the resulting carbons. The review also analysed blending ratios of biomass and plastics, showing their role in balancing porosity and graphitization, which improves electrochemical performance. Key material properties such as surface area, pore volume, and functional groups were examined, with evidence linking these features to charge storage and cycling stability. Electrochemical studies demonstrated that waste-derived carbons can achieve competitive or superior capacity compared to graphite, with hybrid anode (Metal Oxide, Silicon or MXenes) improving the rate capability and sustainability advantages. Challenges identified include low ICE, optimizing blends, and scaling up processes for industrial use. Future perspectives point to pre-lithiation methods, multi-heteroatom co-doping and AI-assisted design with performance outcomes and strategies for commercialization. This study provides clear direction on how waste-derived carbons can transition from laboratory experiments to practical lithium-ion battery applications.

CRediT authorship contribution statement

Adewale George Adeniyi: Writing – review & editing, Visualization, Validation, Formal analysis, Data curation. **Joshua Emeghai:** Writing – review & editing, Writing – original draft, Validation. **Ebuka Chizitere Emenike:** Writing – original draft, Visualization, Investigation, Data curation. **Kingsley O. Iwuozor:** Writing – original draft, Data curation, Conceptualization. **Abdulafeez O. Orilonise:** Formal analysis, Data curation.

Consent for publication

The authors have unanimously decided that this manuscript be sent for possible publication.

Consent to publish

Not applicable.

Compliance with ethical standards

This article does not contain any studies involving human or animal subjects.

Ethics approval and consent to participate

Not applicable.

Data availability

Data sharing is not applicable to this article as no new data were created or analyzed in this study.

Declaration of Competing Interest

The authors declare that they have no known competing financial interests or personal relationships that could have appeared to influence the work reported in this paper.

References

[1] P. Parvizi, M. Jalilian, A.M. Amidi, M.R. Zangeneh, J.-R. Riba, From present innovations to future potential: the promising journey of lithium-ion batteries, Micromachines 16 (2) (2025) 194.
[2] J. Zhao, B. Wang, Z. Zhan, M. Hu, F. Cai, K. Świerczek, K. Yang, J. Ren, Z. Guo, Z. Wang, Boron-doped three-dimensional porous carbon framework/carbon shell encapsulated silicon composites for high-performance lithium-ion battery anodes, J. Colloid Interface Sci. 664 (2024) 790–800.
[3] M.M. Rahman, U. Nisar, A. Abouimrane, I. Belharouak, R. Amin, Valuation of anode materials for high-performance lithium batteries: from graphite to lithium metal and beyond, Electrochem. Energy Rev. 8 (1) (2025) 14.
[4] D. Hu, L. Chen, J. Tian, Y. Su, N. Li, G. Chen, Y. Hu, Y. Dou, S. Chen, F. Wu, Research progress of lithium plating on graphite anode in lithium-ion batteries, Chin. J. Chem. 39 (1) (2021) 165–173.
[5] W. Cai, C. Yan, Y.X. Yao, L. Xu, X.R. Chen, J.Q. Huang, Q. Zhang, The boundary of lithium plating in graphite electrode for safe lithium-ion batteries, Angew. Chem. Int. Ed. 60 (23) (2021) 13007–13012.

[6] Y. Liu, H. Shi, Z.-S. Wu, Recent status, key strategies and challenging perspectives of fast-charging graphite anodes for lithium-ion batteries, Energy Environ. Sci. 16 (11) (2023) 4834–4871.
[7] K.O. Iwuozor, K.P. Odimayomi, E.C. Emenike, H.K. Okoro, S.S. Emmanuel, V.T. Amusa, A.G. Adeniyi, Valorisation of bamboo stalk waste: eco-friendly synthesis and characterisation of activated carbon monolith, Indian Chem. Eng. 67 (2) (2025) 217–230.
[8] A.G. Adeniyi, K.O. Iwuozor, E.C. Emenike, P.A. Sagboye, K.T. Micheal, T.T. Micheal, O.D. Saliu, R. James, Biomass-derived activated carbon monoliths: a review of production routes, performance, and commercialization potential, J. Clean. Prod. (2023) 138711.
[9] C.J. Okorie, T. Ojeyemi, A. Egbemhenghe, M.Q. Ali, E.C. Emenike, K.O. Iwuozor, A.G. Adeniyi, Modification of activated carbon for enhanced treatment of per-and polyfluoroalkyl substances: A focused review, Remediat. J. 34 (2) (2024) e21777.
[10] A. Adeniyi, K. Odimayomi, E.C. Emenike, K. Iwuozor, M. Ndagi, Preparation of activated carbon monolith from waste biomass using solvated polystyrene-based binder, Adv. Mater. Process. Technol. 9 (2023) 1–13.
[11] K.G. Akpomie, K.A. Adegoke, K.O. Oyedotun, J.O. Ighalo, J.F. Amaku, C. Olisah, A.O. Adeola, K.O. Iwuozor, J. Conradie, Removal of bromophenol blue dye from water onto biomass, activated carbon, biochar, polymer, nanoparticle, and composite adsorbents, Biomass. Convers. Biorefinery 14 (2024) 13629–13657.
[12] C.A. Igwegbe, J.O. Ighalo, K.O. Iwuozor, O.D. Onukwuli, A.G. Adeniyi, Response Surface Modelling and Optimisation of Activated Carbons Adsorption of Pollutants from Textile Wastewater, Handbook of Porous Carbon Materials, Springer, Singapore, 2023, pp. 571–593.
[13] A.G. Adeniyi, K.O. Iwuozor, E.C. Emenike, O.J. Ajala, S. Ogunniyi, K.B. Muritala, Thermochemical co-conversion of biomass-plastic waste to biochar: a review, Green. Chem. Eng. 5 (1) (2024) 31–49.
[14] A.G. Adeniyi, V.T. Amusa, E.C. Emenike, K.O. Iwuozor, Hybrid biochar production from biomass and pigmented plastic for sustainable waste-to-energy, Emergent Mater. 6 (2023) 1481–1490.
[15] L. Jin, C.-G. Shen, Q. Wu, A. Shellikeri, J. Zheng, C. Zhang, J. Zheng, Pre-Lithiation strategies for next-generation practical lithium-ion batteries, Adv. Sci. 8 (2021).
[16] P. Molaiyan, G.S. Dos Reis, D. Karuppiah, C.M. Subramaniyam, F. Garcia-Alvarado, U. Lassi, Recent progress in biomass-derived carbon materials for Li-ion and Na-ion batteries—A review, Batteries 9 (2) (2023) 116.
[17] C. Jin, J. Nai, O. Sheng, H. Yuan, W. Zhang, X. Tao, X.W.D. Lou, Biomass-based materials for green lithium secondary batteries, Energy Environ. Sci. 14 (3) (2021) 1326–1379.
[18] Z. Ma, L. Wang, Z. Wang, H. Cui, E. Tang, H. Hou, G. Xu, T. Song, Q. Wang, Recent advances of plastic waste-derived carbon materials for energy storage, environmental remediation and organic synthesis applications, ChemCatChem 16 (23) (2024) e202401072.
[19] L. Yaqoob, T. Noor, N. Iqbal, Conversion of plastic waste to carbon-based compounds and application in energy storage devices, ACS Omega 7 (16) (2022) 13403–13435.
[20] S. Leuthner, Lithium-ion battery overview, in Lithium-Ion Batteries: Basics and Applications, Springer, 2018, pp. 13–19.
[21] Z. Lou, Y. Zhang, Y. Li, L. Xu, Study on microscopic physical and chemical properties of biomass materials by AFM, J. Mater. Res. Technol. 24 (2023) 10005–10026.
[22] H. Tan, C. Lee, P. Ong, K. Wong, C. Bong, C. Li, Y. Gao, A review on the comparison between slow pyrolysis and fast pyrolysis on the quality of lignocellulosic and lignin-based biochar, in IOP Conference Series: Materials Science and Engineering, IOP Publishing, 2021.
[23] C. Chen, K. Sun, C. Huang, M. Yang, M. Fan, A. Wang, G. Zhang, B. Li, J. Jiang, W. Xu, Investigation on the mechanism of structural reconstruction of biochars derived from lignin and cellulose during graphitization under high temperature, Biochar 5 (1) (2023) 51.
[24] K. Xu, Y. Li, J. Xiong, X. Ou, W. Su, G. Zhong, C. Yang, Activated amorphous carbon with high-porosity derived from camellia pollen grains as anode materials for lithium/sodium ion batteries, Front. Chem. 6 (2018) 366.
[25] M.M. Alam, M.A. Hossain, M.D. Hossain, M. Johir, J. Hossen, M.S. Rahman, J.L. Zhou, A.K. Hasan, A.K. Karmakar, M.B. Ahmed, The potentiality of rice husk-derived activated carbon: From synthesis to application, Processes 8 (2) (2020) 203.
[26] S. Kumagai, Y. Abe, M. Tomioka, M. Kabir, Suitable binder for Li-ion battery anode produced from rice husk, Sci. Rep. 11 (1) (2021) 15784.
[27] D. Bhatia, A.K. Saroha, Rice straw-derived biochar as anode material for lithium-ion battery: a step toward sustainable development, Energy Technol. 12 (6) (2024) 2400096.
[28] P. Yan, F. Ai, C. Cao, Z. Luo, Hierarchically porous carbon derived from wheat straw for high rate lithium ion battery anodes, J. Mater. Sci. Mater.Electron. 30 (15) (2019) 14120–14129.
[29] C.A. Mullen, A.A. Boateng, N.M. Goldberg, I.M. Lima, D.A. Laird, K.B. Hicks, Bio-oil and bio-char production from corn cobs and stover by fast pyrolysis, Biomass. bioenergy 34 (1) (2010) 67–74.
[30] L. Zhu, H. Lei, L. Wang, G. Yadavalli, X. Zhang, Y. Wei, Y. Liu, D. Yan, S. Chen, B. Ahring, Biochar of corn stover: microwave-assisted pyrolysis condition induced changes in surface functional groups and characteristics, J. Anal. Appl. Pyrolysis 115 (2015) 149–156.
[31] A.E. Barruna, R.M. Naufal, M.R. Nugraha, I. Subiyanto, N. Tinaprilla, A. Subhan, H. Chairul, Material characteristics and electrochemical performance of lithium-ion capacitor with activated carbon cathode derived from sugarcane bagasse, in IOP Conference Series: Earth and Environmental Science, IOP Publishing, 2021.
[32] T. Mimmo, P. Panzacchi, M. Baratieri, C. Davies, G. Tonon, Effect of pyrolysis temperature on miscanthus (Miscanthus× giganteus) biochar physical, chemical and functional properties, Biomass. Bioenergy 62 (2014) 149–157.
[33] A. Singh, S. Nanda, J.F. Guayaquil-Sosa, F. Berruti, Pyrolysis of Miscanthus and characterization of value-added bio-oil and biochar products, Can. J. Chem. Eng. 99 (2021) S55–S68.
[34] M. Brebu, S. Ucar, C. Vasile, J. Yanik, Co-pyrolysis of pine cone with synthetic polymers, Fuel 89 (8) (2010) 1911–1918.
[35] P. Lu, Q. Huang, A.T. Bourtsalas, Y. Chi, J. Yan, Synergistic effects on char and oil produced by the co-pyrolysis of pine wood, polyethylene and polyvinyl chloride, Fuel 230 (2018) 359–367.
[36] C. Xia, C. Kang, M.D. Patel, L. Cai, B. Gwalani, R. Banerjee, S.Q. Shi, W. Choi, Pine wood extracted activated carbon through self-activation process for high-performance lithium-ion battery, ChemistrySelect 1 (13) (2016) 4000–4007.
[37] M.J.B. Nogueira, S. Chauque, V. Sperati, L. Savio, G. Divitini, L. Pasquale, S. Marras, P. Franchi, S. Paciornik, R.P. Zaccaria, Untreated bamboo biochar as anode material for sustainable lithium ion batteries, Biomass. Bioenergy 193 (2025) 107511.
[38] E. Taer, M. Deraman, I. Talib, A. Awitdrus, S. Hashmi, A. Umar, Preparation of a highly porous binderless activated carbon monolith from rubber wood sawdust by a multi-step activation process for application in supercapacitors, Int. J. Electrochem. Sci. 6 (8) (2011) 3301–3315.
[39] M. Paul, A. Grimm, G. Simões Dos Reis, G. Manavalan, S. ES, M. Thyrel, S. Petnikota, Activated carbon from birch wood as an electrode material for aluminum batteries and supercapacitors, ChemElectroChem 12 (4) (2025) e202400549.
[40] M. Maharjan, N. Wai, A. Veksha, A. Giannis, T.M. Lim, G. Lisak, Sal wood sawdust derived highly mesoporous carbon as prospective electrode material for vanadium redox flow batteries, J. Electroanal. Chem. 834 (2019) 94–100.
[41] A.G. Adeniyi, E.C. Emenike, A.O. Ezzat, K.O. Iwuozor, O.H. Abd-Elkader, H.A. Al-Lohedan, T. Ojeyemi, H.B. Saka, S.S. Emmanuel, Investigating the properties and agronomic benefits of onion peel and chicken feather-derived biochars, Heliyon 10 (15) (2024).
[42] J. Liu, S. Huang, K. Chen, T. Wang, M. Mei, J. Li, Preparation of biochar from food waste digestate: pyrolysis behavior and product properties, Bioresour. Technol. 302 (2020) 122841.
[43] V. Pelagalli, M. Langone, S. Matassa, M. Race, R. Tuffi, S. Papirio, P.N. Lens, M. Lazzazzara, A. Frugis, L. Petta, Pyrolysis of municipal sewage sludge: challenges, opportunities and new valorization routes for biochar, bio-oil, and pyrolysis gas, Environmental Science Water Research Technology 10 (10) (2024) 2282–2312.
[44] B. Chen, Z. Gu, M. Wu, Z. Ma, H.R. Lim, K.S. Khoo, P.L. Show, Advancement pathway of biochar resources from macroalgae biomass: a review, Biomass. Bioenergy 167 (2022) 106650.
[45] P. Salimi, O. Norouzi, S. Pourhoseini, P. Bartocci, A. Tavasoli, F. Di Maria, S. Pirbazari, G. Bidini, F. Fantozzi, Magnetic biochar obtained through catalytic pyrolysis of macroalgae: a promising anode material for Li-ion batteries, Renew. Energy 140 (2019) 704–714.
[46] R.K. Mishra, Co-pyrolysis of low-value wood sawdust and non-recyclable plastics into char: effect of plastic loading on char yield and its properties, RSC Sustain. 3 (4) (2025) 1774–1787.
[47] J. Huang, X. Lin, W. Zhang, L. Guan, J. Xu, J. Gu, Y. Zhou, C. Hu, Cell wall composition of Camellia oleifera Abel. shell: new insights into its composition distribution and ultrastructure, Holzforschung 78 (6) (2024) 317–328.
[48] Y. Liu, T. Sun, D. Ege, A.R. Kamali, Cobalt oxide-decorated on carbon derived from onion skin biomass for Li-ion storage application, Metals 14 (2) (2024) 191.
[49] F. Luna-Lama, J. Morales, A. Caballero, Biomass porous carbons derived from banana peel waste as sustainable anodes for lithium-ion batteries, Materials 14 (20) (2021) 5995.
[50] H. Wan, X. Hu, Nitrogen doped biomass-derived porous carbon as anode materials of lithium ion batteries, Solid State Ion. (2019).
[51] S.D. Stefanidis, E. Heracleous, D.T. Patiaka, K.G. Kalogiannis, C.M. Michailof, A.A. Lappas, Optimization of bio-oil yields by demineralization of low quality biomass, Biomass. Bioenergy 83 (2015) 105–115.
[52] A.K. Kumar, B.S. Parikh, M. Pravakar, Natural deep eutectic solvent mediated pretreatment of rice straw: bioanalytical characterization of lignin extract and enzymatic hydrolysis of pretreated biomass residue, Environ. Sci. Pollut. Res. 23 (10) (2016) 9265–9275.
[53] G.J. de Moraes Rocha, V.M. Nascimento, A.R. Goncalves, V.F.N. Silva, C. Martín, Influence of mixed sugarcane bagasse samples evaluated by elemental and physical–chemical composition, Ind. Crops Prod. 64 (2015) 52–58.
[54] R. Moriana, F. Vilaplana, M. Ek, Forest residues as renewable resources for bio-based polymeric materials and bioenergy: chemical composition, structure and thermal properties, Cellulose 22 (5) (2015) 3409–3423.
[55] R. Saidur, E. Abdelaziz, A. Demirbas, M.S. Hossain, S. Mekhilef, A review on biomass as a fuel for boilers, Renew. Sustain. Energy Rev. 15 (5) (2011) 2262–2289.
[56] F. Talebnia, D. Karakashev, I. Angelidaki, Production of bioethanol from wheat straw: an overview on pretreatment, hydrolysis and fermentation, Bioresour. Technol. 101 (13) (2010) 4744–4753.
[57] M. Faye, S. Ndiaye, G. Vilarem, O. Sock, L. Rigal, Chemical characterisation of the Senegalese neem seed: Distribution of the main constituents, Azadirachtins Lipids Proteins Fibers (Cellul. Hemicellul. lignin) (2010).
[58] D. Rathnayake, P.O. Ehidiamhen, C.E. Egene, C.V. Stevens, E. Meers, O. Mašek, F. Ronsse, Investigation of biomass and agricultural plastic co-pyrolysis: effect on biochar yield and properties, J. Anal. Appl. Pyrolysis 155 (2021) 105029.
[59] P. Zhang, Y. Shu, B. Zhong, L. Yang, X. Guo, Optimizing sodium storage mechanisms and electrochemical performance of high Nitrogen-Doped hard carbon anode materials Derived from waste plastics for Sodium-Ion batteries, Chem. Eng. J. 498 (2024) 155231.

[60] J. Jiang, L. Zhang, X. Wang, N. Holm, K. Rajagopalan, F. Chen, S. Ma, Highly ordered macroporous woody biochar with ultra-high carbon content as supercapacitor electrodes, Electrochim. Acta 113 (2013) 481–489.
[61] J. Deng, B. Yi, O. Mašek, X. Yuan, S.Y. Hwang, H.C. Ong, Z. Hua, Y.S. Ok, Co-pyrolysis of biomass and plastic waste into carbon materials with environmental applications: a critical review, Green. Chem. (2025).
[62] B. Qiu, M. Liu, X. Qu, B. Zhang, H. Xie, D. Wang, L. Lee, H. Yin, Recycling Spent Lithium-Ion Batteries Using Waste Benzene-Containing Plastics: Synergetic Thermal Reduction and Benzene Decomposition, Environmental science & technology, 2023.
[63] Q. Zhang, D. Zhang, W. Lu, M.U. Khan, H. Xu, W. Yi, H. Lei, E. Huo, M. Qian, Y. Zhao, Production of high-density polyethylene biocomposites from rice husk biochar: Effects of varying pyrolysis temperature, Sci. Total Environ. 738 (2020) 139910.
[64] K.T. Kumar, S. Raghu, A. Shanmugharaj, Transmogrifying waste blister packs into defect-engineered graphene-like turbostratic carbon: novel lithium-ion (Li-ion) battery anode with noteworthy electrochemical characteristics, Nanoscale 14 (11) (2022) 4312–4323.
[65] M.A.A.M. Abdah, F.N.M. Azlan, W. Wong, M.N. Mustafa, R. Walvekar, M. Khalid, Microwave-assisted upcycling of plastic waste to high-performance carbon anode for lithium-ion batteries, Chemosphere (2023) 140973.
[66] C. Ehi-Eromosele, C. Onwucha, S. Ajayi, G. Melinte, A.L. Hansen, S. Indris, H. Ehrenberg, Ionothermal synthesis of activated carbon from waste PET bottles as anode materials for lithium-ion batteries, RSC Adv. 12 (2022) 34670–34684.
[67] B.B. Uzoejinwa, X. He, S. Wang, A.E.-F. Abomohra, Y. Hu, Z. He, Q. Wang, Co-pyrolysis of seaweeds with waste plastics: modeling and simulation of effects of co-pyrolysis parameters on yields, and optimization studies for maximum yield of enhanced biofuels, Energy Source Part A Recovery Util. Environ. Eff. 42 (8) (2020) 954–978.
[68] H. Weldekidan, A.K. Mohanty, M. Misra, Upcycling of plastic wastes and biomass for sustainable graphitic carbon production: a critical review, ACS Environ. Au 2 (6) (2022) 510–522.
[69] M. Gale, P.M. Nguyen, K.L. Gilliard-AbdulAziz, Synergistic and antagonistic effects of the co-pyrolysis of plastics and corn stover to produce char and activated carbon, ACS Omega 8 (1) (2022) 380–390.
[70] N. Wantaneeyakul, K. Kositkanawuth, S.Q. Turn, J. Fu, Investigation of biochar production from copyrolysis of rice husk and plastic, ACS Omega 6 (43) (2021) 28890–28902.
[71] J. Li, F. Dou, J. Gong, Y. Gao, Y. Hua, K. Sielicki, D. Zhang, E. Mijowska, X. Chen, Recycling of plastic wastes for the mass production of yolk–shell-nanostructured Co3O4@C for lithium-ion batteries, ACS Appl. Nano Mater. (2023).
[72] T. Wei, Z. Zhang, Z. Zhu, X. Zhou, Y. Wang, Y. Wang, Q. Zhuang, Recycling of waste plastics and scalable preparation of Si/CNF/C composite as anode material for lithium-ion batteries, Ionics 25 (4) (2019) 1523–1529.
[73] L. Chen, S. Wang, H. Meng, Z. Wu, J. Zhao, Synergistic effect on thermal behavior and char morphology analysis during co-pyrolysis of paulownia wood blended with different plastics waste, Appl. Therm. Eng. 111 (2017) 834–846.
[74] W. Zhang, J. Yin, Z. Lin, H. Lin, H. Lu, Y. Wang, W. Huang, Facile preparation of 3D hierarchical porous carbon from lignin for the anode material in lithium ion battery with high rate performance, Electrochim. Acta 176 (2015) 1136–1142.
[75] A. Dewangan, D. Pradhan, R. Singh, Co-pyrolysis of sugarcane bagasse and low-density polyethylene: influence of plastic on pyrolysis product yield, Fuel 185 (2016) 508–516.
[76] P.N.Y. Yek, Y.H. Chan, S.Y. Foong, W.A.W. Mahari, X. Chen, R.K. Liew, N.L. Ma, Y.F. Tsang, C. Sonne, Y.W. Cheng, Co-processing plastics waste and biomass by pyrolysis–gasification: a review, Environ. Chem. Lett. 22 (1) (2024) 171–188.
[77] G. Shen, B. Li, Y. Xu, X. Chen, S. Katiyar, L.-M. Zhu, L. Xie, Q. Han, X. Qiu, X. Wu, X. Cao, Waste biomass garlic stem-derived porous carbon materials as high-capacity and long-cycling anode for lithium/sodium-ion batteries, J. Colloid Interface Sci. 653 (2023) 1588–1599 (Pt B).
[78] L. Tao, Y. Huang, Y. Zheng, X. Yang, C. Liu, M. Di, S. Larpkiattaworn, M. Nimlos, Z. Zheng, Porous carbon nanofiber derived from a waste biomass as anode material in lithium-ion batteries, J. Taiwan Inst. Chem. Eng. (2019).
[79] H. Darjazi, L. Bottoni, H. Moazami, S. Rezvani, L. Balducci, L. Sbrascini, A. Staffolani, A. Tombesi, F. Nobili, From waste to resources: transforming olive leaves to hard carbon as sustainable and versatile electrode material for Li/Na-ion batteries and supercapacitors, Mater. Today Sustain. 21 (2023) 100313.
[80] F. Zheng, D. Liu, G. Xia, Y. Yang, T. Liu, M. Wu, Q. Chen, Biomass waste inspired nitrogen-doped porous carbon materials as high-performance anode for lithium-ion batteries, J. Alloy. Compd. 693 (2017) 1197–1204.
[81] C. Senthil, C.W. Lee, Biomass-derived biochar materials as sustainable energy sources for electrochemical energy storage devices, Renew. Sustain. Energy Rev. 137 (2021) 110464.
[82] Y. Cheng, J. Wang, C. Fang, Y. Du, J. Su, J. Chen, Y. Zhang, Recent progresses in pyrolysis of plastic packaging wastes and biomass materials for conversion of high-value carbons: a review, Polymers 16 (8) (2024) 1066.
[83] K. Sharma, P. Kadyan, R.K. Sharma, S. Grover, Heteroatom doping in bio-waste derived activated carbon for enhanced supercapacitor performance: a review, J. Energy Storage 100 (2024) 113679.
[84] L. Tao, Y. Huang, Y. Zheng, X. Yang, C. Liu, M. Di, S. Larpkiattaworn, M.R. Nimlos, Z. Zheng, Porous carbon nanofiber derived from a waste biomass as anode material in lithium-ion batteries, J. Taiwan Inst. Chem. Eng. 95 (2019) 217–226.
[85] L. Xie, C. Tang, Z. Bi, M. Song, Y. Fan, C. Yan, X. Li, F. Su, Q. Zhang, C. Chen, Hard carbon anodes for next-generation Li-ion batteries: review and perspective, Adv. Energy Mater. 11 (38) (2021) 2101650.
[86] H. Tran Thi Dieu, K. Charoensook, H.-C. Tai, Y.-T. Lin, Y.-Y. Li, Preparation of activated carbon derived from oil palm empty fruit bunches and its modification by nitrogen doping for supercapacitors, J. Porous Mater. 28 (1) (2021) 9–18.
[87] S. Hongthong, W. Sangsida, S. Wongcharee, A. Chanthakhot, P. Aungthitipan, K. Suwannahong, T. Kreetachat, J. Rioyo, Enhanced biochar production via co-pyrolysis of biomass residual with plastic waste after recycling process, Int. J. Chem. Eng. 2024 (1) (2024) 1176275.
[88] Y. Gao, Q. Yue, B. Gao, A. Li, Insight into activated carbon from different kinds of chemical activating agents: a review, Sci. Total Environ. 746 (2020) 141094.
[89] N.L. Panwar, A. Pawar, Influence of activation conditions on the physicochemical properties of activated biochar: a review, Biomass. Convers. Biorefinery 12 (3) (2022) 925–947.
[90] P. Dubey, V. Shrivastav, P.H. Maheshwari, S. Sundriyal, Recent advances in biomass derived activated carbon electrodes for hybrid electrochemical capacitor applications: challenges and opportunities, Carbon 170 (2020) 1–29.
[91] G.M. Kalu-Uka, S. Kumar, A.C. Kalu-Uka, S. Vikram, G.O. Ihekweme, N. Ranjan, E.N. Anosike-Francis, G. Prajapati, A. Nduba, A.P. Onwualu, Production of activated carbon electrode for energy storage application in supercapacitors via KOH activation of waste termite biomass, Waste Biomass. Valoriz. (2022) 1–16.
[92] M. Adibfar, T. Kaghazchi, N. Asasian, M. Soleimani, Conversion of poly (ethylene terephthalate) waste into activated carbon: chemical activation and characterization, Chem. Eng. Technol. 37 (6) (2014) 979–986.
[93] A.G. Adeniyi, K.O. Iwuozor, E.C. Emenike, S. Ogunniyi, M.A. Amoloye, P.A. Sagboye, One-step chemical activation for the production of engineered orange peel biochar, Emergent Mater. 6 (2022) 211–221.
[94] J. Wang, S. Kaskel, KOH activation of carbon-based materials for energy storage, J. Mater. Chem. 22 (45) (2012) 23710–23725.
[95] B.S. Girgis, A.-N.A. El-Hendawy, Porosity development in activated carbons obtained from date pits under chemical activation with phosphoric acid, Microporous Mesoporous Mater. 52 (2) (2002) 105–117.
[96] A. Kwaghger, J. Ibrahim, Optimization of conditions for the preparation of activated carbon from mango nuts using HCl, Am. J. Eng. Res. 2 (7) (2013) 74–85.
[97] A.G. Adeniyi, K.O. Iwuozor, E.C. Emenike, M.A. Amoloye, E.S. Aransiola, F.O. Motolani, S.H. Kayode, Prospects and problems in the development of biochar-filled plastic composites: a review, Funct. Compos. Struct. 5 (1) (2023) 012002.
[98] R. Boonprachai, T. Autthawong, O. Namsar, C. Yodbunork, W. Yodying, T. Sarakonsri, Natural porous carbon derived from popped rice as anode materials for lithium-ion batteries, Crystals 12 (2) (2022) 223.
[99] W. Sari, A. Arnelli, Y. Astuti, The effect of activated carbon and Lithium titanate ratio on the electrochemical performance of Lithium-Ion battery anode, in AIP Conference Proceedings, AIP Publishing LLC, 2024.
[100] N.A. Barakat, O.M. Irfan, H.M. Moustafa, H3PO4/KOH activation agent for high performance rice husk activated carbon electrode in acidic media supercapacitors, Molecules 28 (1) (2022) 296.
[101] W. Lv, F. Wen, J. Xiang, J. Zhao, L. Li, L. Wang, Z. Liu, Y. Tian, Peanut shell derived hard carbon as ultralong cycling anodes for lithium and sodium batteries, Electrochim. Acta 176 (2015) 533–541.
[102] W. Li, X. Lu, B.W. Biney, J. Li, Y. Yan, K. Chen, In-situ synthesis of heteroatom-doped hard carbon for sodium-ion batteries: Dual benefits for green energy and environment, J. Colloid Interface Sci. 677 (2025) 312–322.
[103] D. Bosubabu, R. Sampathkumar, G. Karkera, K. Ramesha, Facile approach to prepare multiple heteroatom-doped carbon material from bagasse and its applications toward lithium-ion and lithium–sulfur batteries, Energy Fuels 35 (9) (2021) 8286–8294.
[104] N. Kietisirirojana, T. Tunkasiri, K. Pengpat, O. Khamman, U. Intatha, S. Eitssayeam, Synthesis of mesoporous carbon powder from gold beard grass pollen for use as an anode for lithium-ion batteries, Microporous Mesoporous Mater. 331 (2022) 111565.
[105] D. Vernardou, G. Psaltakis, T. Tsubota, N. Katsarakis, D. Kalderis, Challenges and perspectives of biochar anodes for lithium-ion batteries, Future Batter. 4 (2024) 100011.
[106] O.E. Eleri, F. Lou, Z. Yu, Lithium-ion capacitors: a review of strategies toward enhancing the performance of the activated carbon cathode, Batteries 9 (11) (2023) 533.
[107] X. Zhao, Y. Chen, H. Sun, T. Yuan, Y. Gong, X. Liu, T. Chen, Impact of surface structure on sei for carbon materials in alkali ion batteries: a review, Batteries 9 (4) (2023) 226.
[108] F. Ahmed, G. Almutairi, P.M. Hasan, S. Rehman, S. Kumar, N.M. Shaalan, A. Aljaafari, A. Alshoaibi, B. AlOtaibi, K. Khan, Fabrication of a biomass-derived activated carbon-based anode for high-performance li-ion batteries, Micromachines 14 (1) (2023) 192.
[109] I. Alouiz, M. Aqil, M. Dahbi, M.Y. Amarouch, D. Mazouzi, Performance of high-energy storage activated carbon derived from olive pomace biomass as an anode material for sustainable lithium-ion batteries, Resour. Chem. Mater. 4 (2) (2025) 100086.
[110] R. Joia, M. Atamanov, K. Umbetkaliev, M. Mohammadi, S. Sarwari, T. Modaqeq, Exploring the versatile production techniques and applications of nitrogen-doped activated carbon, Therm. Sci. Eng. 7 (1) (2024) 1–26.
[111] Yeskozha, D., A. Zhanaikhan, A. Sarsengaliyeva, and A. Nurpeissova, Enhanced electrochemical performance of phosphorus-doped hard carbon anodes derived from upcycled PET-bottles for lithium-ıon batteries.
[112] J. Yu, X. Wang, J. Peng, X. Jia, L. Li, X. Chuan, Porous activity of biomass-activated carbon enhanced by nitrogen-dopant towards high-performance lithium ion hybrid battery-supercapacitor, J. Electrochem. Soc. 168 (12) (2021) 120537.
[113] T. Ramachandran, F. Hamed, Y.A. Kumar, R.K. Raji, H. Hegazy, Multifunctional covalent-organic frameworks (COFs)-2D MXenes composites for diverse applications, J. Energy Storage 73 (2023) 109299.

[114] L. Xie, G. Shen, B. Li, J. Zhou, L.-M. Zhu, Q. Han, X. Qiu, X. Cao, Porous carbon materials derived from waste tea leaves as high-capacity anodes for lithium/sodium ion batteries, J. Energy Storage (2024).
[115] G.D. Reis, C. Subramaniyam, A. Grimm, M. Hamedi, P. Molaiyan, F. García-Alvarado, U. Lassi, J. Goclon, S. Petnikota, Biomass-derived macroporous carbon-tin oxide composites as stable and high-capacity anodes for lithium-ion and sodium-ion batteries: experimental study and GFN1-xTB calculations. Physical chemistry chemical physics, PCCP (2025).
[116] J. Hosseinzadeh, S. Mahdavi, A. Ashori, A. Spitsyn, Synthesis and characterization of hierarchically porous carbon anodes from furfural biorefinery residues for sustainable lithium-ion batteries, J. Anal. Appl. Pyrolysis (2024).
[117] F. Ahmed, G. Almutairi, P. Hasan, S. Rehman, S. Kumar, N. Shaalan, A. Aljaafari, A. Alshoaibi, B. AlOtaibi, K. Khan, Fabrication of a biomass-derived activated carbon-based anode for high-performance Li-Ion batteries, Micromachines 14 (2023).
[118] H. Shang, X. Hao, Y. Zhou, J. Peng, L. Guo, H. Li, B. Sun, Activated carbon from spartina alterniflora and its N-doped material for Li-Ion Battery Anode, Nanomaterials 15 (2025).
[119] G. Liu, Y. Zhao, J. Li, T. Zhang, M. Yang, D. Guo, N. Wu, K. Wu, X. Liu, Hierarchical N/O co-doped hard carbon derived from waste Saccharomyces cerevisiae for lithium storage, J. Electroanal. Chem. (2022).
[120] O.M. Mutiat, A. Alpysbayev, D. Abduakhitov, K. Kudaibergenov, Z. Bakenov, S.T. Myung, A. Konarov, Effect of pre-treatment conditions on the electrochemical performance of hard carbon derived from bio-waste, RSC Adv. 15 (2025) 1105–1114.
[121] A. Gomez-Martin, J. Martínez-Fernández, M. Ruttert, M. Winter, T. Placke, J. Ramirez-Rico, An electrochemical evaluation of nitrogen-doped carbons as anodes for lithium ion batteries, Carbon (2020).
[122] T. Ramachandran, F. Hamed, R.K. Raji, S.M. Majhi, D. Barik, Y.A. Kumar, R.M. Jauhar, M. Pachamuthu, L. Vijayalakshmi, S. Ansar, Enhancing asymmetric supercapacitor performance with NiCo2O4–NiO hybrid electrode fabrication, J. Phys. Chem. Solids 180 (2023) 111467.
[123] Z. Guo, Z. Liu, W. Chen, X. Sun, X. Zhang, K. Wang, Y. Ma, Battery-type lithium-ion hybrid capacitors: current status and future perspectives, batteries 9 (2) (2023) 74.
[124] W. Lin, S. Zhao, B. Lu, F. Jiang, Z. Lu, Z. Xu, Structures, performances and applications of green biomass derived carbon in lithium-ion batteries, Energy Mater. 4 (5) (2024) (p. N/A-N/A).
[125] X. Ji, Y. Wei, H. Yang, Z. Lu, S. Jin, H. Jin, X. Kong, H. Ji, Extended Plateau Capacity of Hard Carbon Anode for High Energy Lithium-Ion Batteries, Small 20 (42) (2024) 2402616.
[126] R. Muruganantham, F.-M. Wang, R.A. Yuwono, M. Sabugaa, W.-R. Liu, Biomass feedstock of waste mango-peel-derived porous hard carbon for sustainable high-performance lithium-ion energy storage devices, Energy Fuels 35 (13) (2021) 10878–10889.
[127] Q. Zhou, W. Yang, L. Wang, H. Lu, S. Nie, L. Xu, W. Yang, C. Wei, Biomass carbon materials for high-performance secondary battery electrodes: a review, Resour. Chem. Mater. 3 (2) (2024) 123–145.
[128] M. González-Hourcade, G.S. dos Reis, A. Grimm, V.M. Dinh, E.C. Lima, S.H. Larsson, F.G. Gentili, Microalgae biomass as a sustainable precursor to produce nitrogen-doped biochar for efficient removal of emerging pollutants from aqueous media, J. Clean. Prod. 348 (2022) 131280.
[129] T. Ramachandran, R.K. Raji, S. Palanisamy, N. Renuka, K. Karuppasamy, The role of in situ and operando techniques in unraveling local electrochemical supercapacitor phenomena, J. Ind. Eng. Chem. 145 (2025) 144–168.
[130] X. Zhou, H. Li, J. Yang, Biomass-derived activated carbon materials with plentiful heteroatoms for high-performance electrochemical capacitor electrodes, J. Energy Chem. 25 (1) (2016) 35–40.
[131] C. Liao, S. Wu, Pseudocapacitance behavior on Fe3O4-pillared SiOx microsphere wrapped by graphene as high performance anodes for lithium-ion batteries, Chem. Eng. J. 355 (2019) 805–814.
[132] P. Liang, Z. Huo, Y. Liu, Z. Bo, Y. Wu, X. Hu, Z. Wen, Biomass-Derived Phosphorus-Doped Porous Hard Carbon Anode for Stable and High-Rate Sodium Ion Batteries, Batter. Supercaps 8 (6) (2025) e202400694.
[133] J.S. Gnanaraj, R.J. Lee, A.M. Levine, J.L. Wistrom, S.L. Wistrom, Y. Li, J. Li, K. Akato, A.K. Naskar, M.P. Paranthaman, Sustainable waste tire derived carbon material as a potential anode for lithium-ion batteries, Sustainability 10 (8) (2018) 2840.
[134] Z. Tang, R. Zhang, H. Wang, S. Zhou, Z. Pan, Y. Huang, D. Sun, Y.-G. Tang, X. Ji, K. Amine, M. Shao, Revealing the closed pore formation of waste wood-derived hard carbon for advanced sodium-ion battery, Nat. Commun. 14 (2023).
[135] J. Yang, H. Gao, S. Men, Z. Shi, Z. Lin, X. Kang, S. Chen, CoSe2 Nanoparticles Encapsulated by N-Doped Carbon Framework Intertwined with Carbon Nanotubes: High-Performance Dual-Role Anode Materials for Both Li- and Na-Ion Batteries, Adv. Sci. 5 (2018).
[136] H. Chen, N. Sun, Q. Zhu, R. Soomro, B. Xu, Microcrystalline Hybridization Enhanced Coal-Based Carbon Anode for Advanced Sodium-Ion Batteries, Adv. Sci. 9 (2022).
[137] R. Cui, B. Xu, H. Dong, C. Yang, Q. Jiang, N/O Dual-Doped Environment-Friendly Hard Carbon as Advanced Anode for Potassium-Ion Batteries, Adv. Sci. 7 (2020).
[138] R.M. Bhattarai, N. Le, K. Chhetri, D. Acharya, S.M.S. Pandiyarajan, S. Saud, S.J. Kim, Y. Mok, Synergistic Performance Boosts of Dopamine-Derived Carbon Shell Over Bi-metallic Sulfide: A Promising Advancement for High-Performance Lithium-Ion Battery Anodes, Adv. Sci. 11 (2024).
[139] Z. Wang, S. Weng, H. Zhang, L. Wang, X. Yao, H. Tu, D. Huang, S. Lu, L. Liu, J. Xue, F. Zhang, G. Wu, J. Zheng, Q. Wang, L. Chen, J. Xu, H. Li, X. Wu, Balancing anodic stability and cathodic kinetics in practical lithium-sulfur batteries with non-fluorinated weakly solvating solvents, Adv. Sci. (2025).
[140] R. Mo, F. Li, X. Tan, P. Xu, R. Tao, G. Shen, X. Lu, F. Liu, L. Shen, B. Xu, Q. Xiao, X. Wang, C. Wang, J. Li, G. Wang, Y. Lu, High-quality mesoporous graphene particles as high-energy and fast-charging anodes for lithium-ion batteries, Nat. Commun. 10 (2019).
[141] V. Etacheri, C. Hong, V. Pol, Upcycling of packing-peanuts into carbon microsheet anodes for lithium-Ion batteries, Environ. Sci. Technol. 49 (18) (2015) 11191–11198.
[142] G. Simoes dos Reis, C. Mayandi Subramaniyam, A.D. Cárdenas, S.H. Larsson, M. Thyrel, U. Lassi, F. Garcia-Alvarado, Facile synthesis of sustainable activated biochars with different pore structures as efficient additive-carbon-free anodes for lithium-and sodium-ion batteries, ACS Omega 7 (46) (2022) 42570–42581.
[143] S. Weng, G. Yang, S. Zhang, X. Liu, X. Zhang, Z. Liu, M. Cao, M.N. Ateş, Y. Li, L. Chen, Kinetic limits of graphite anode for fast-charging lithium-ion batteries, NanoMicro Lett. 15 (1) (2023) 215.
[144] Y. Zhao, X. Li, B. Yan, D. Xiong, D. Li, S. Lawes, X. Sun, Recent developments and understanding of novel mixed transition-metal oxides as anodes in lithium ion batteries, Adv. Energy Mater. 6 (8) (2016) 1502175.
[145] A.T.A. Ahmed, R. Soni, A.S. Ansari, C.Y. Lee, H.-S. Kim, H. Im, C. Bathula, Biowaste-derived graphitic carbon interfaced TiO2 as anode for lithium-ion battery, Surf. Interfaces 35 (2022) 102404.
[146] H. Ying, W. Han, Metallic Sn-Based Anode Materials: Application in High-Performance Lithium-Ion and Sodium-Ion Batteries, Adv. Sci. 4 (2017).
[147] K. Liang, T. Wu, S. Misra, C. Dun, S. Husmann, K. Prenger, J. Urban, V. Presser, R. Unocic, De Jiang, M. Naguib, *Nitrogen-Doped Graphene-Like Carbon Intercalated MXene Heterostructure Electrodes for Enhanced Sodium- and Lithium-Ion Storage.* Advanced, Science (2024) **11**.
[148] F. Zhou, Z. Li, Y. Lu, B. Shen, Y. Guan, X. Wang, Y.C. Yin, B.S. Zhu, L.-L. Lu, Y. Ni, Y. Cui, H.B. Yao, S. Yu, Diatomite derived hierarchical hybrid anode for high performance all-solid-state lithium metal batteries, Nat. Commun. 10 (2019).
[149] H. Jia, X. Li, J. Song, X. Zhang, L. Luo, Y. He, B. Li, Y. Cai, S. Hu, X. Xiao, C. Wang, K. Rosso, R. Yi, R. Patel, J.G. Zhang, Hierarchical porous silicon structures with extraordinary mechanical strength as high-performance lithium-ion battery anodes, Nat. Commun. 11 (2020).
[150] E. Zhang, X. Jia, B. Wang, J. Wang, X. Yu, B. Lu, Carbon Dots@rGO Paper as Freestanding and Flexible Potassium-Ion Batteries Anode, Adv. Sci. 7 (2020).
[151] S. Ahn, The Development of Activated Carbon from Animal and Plant Biomass Sources for Lithium–Sulfur Battery Applications: A Mini-Review, Coatings 15 (1) (2025) 43.
[152] C. Zhang, S.-H. Park, A. Seral-Ascaso, S. Barwich, N. McEvoy, C. Boland, J. Coleman, Y. Gogotsi, V. Nicolosi, High capacity silicon anodes enabled by MXene viscous aqueous ink, Nat. Commun. 10 (2019).